

PCT

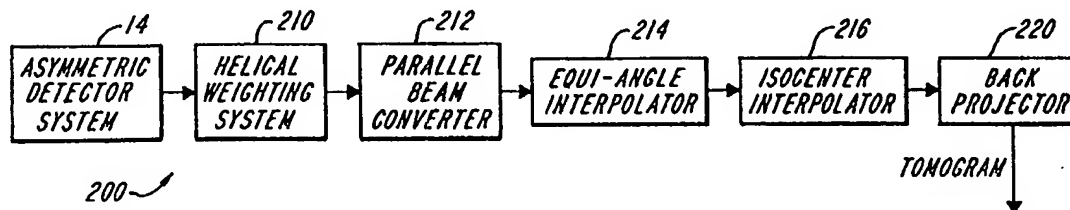
WORLD INTELLECTUAL PROPERTY ORGANIZATION
International Bureau



INTERNATIONAL APPLICATION PUBLISHED UNDER THE PATENT COOPERATION TREATY (PCT)

(51) International Patent Classification ⁶ : A61B 6/03	A1	(11) International Publication Number: WO 98/23209 (43) International Publication Date: 4 June 1998 (04.06.98)
(21) International Application Number: PCT/US97/21036 (22) International Filing Date: 10 November 1997 (10.11.97) (30) Priority Data: 08/759,368 27 November 1996 (27.11.96) US (71) Applicant: ANALOGIC CORPORATION [US/US]; Eight Centennial Drive, Peabody, MA 01960 (US). (72) Inventors: RUTH, Christopher, C.; 23 School Street, Danvers, MA 01923 (US). DOBBS, John, M.; 218 Sagamore Street, Hamilton, MA 01982 (US). CRAWFORD, Carl, R.; Apartment 207, 20 Webster Street, Brookline, MA 02146 (US). (74) Agents: KUSMER, Toby, H. et al.; Lappin & Kusmer LLP, 200 State Street, Boston, MA 02109 (US).		(81) Designated States: BR, CN, DE, JP, KR. Published With international search report.

(54) Title: HELICAL COMPUTED TOMOGRAPHY WITH ASYMMETRIC DETECTOR SYSTEM



(57) Abstract

A computed tomography system (200) and method for reconstructing a tomographic image using an asymmetric detector array (14) during a weighted helical (210) scan.

FOR THE PURPOSES OF INFORMATION ONLY

Codes used to identify States party to the PCT on the front pages of pamphlets publishing international applications under the PCT.

AL	Albania	ES	Spain	LS	Lesotho	SI	Slovenia
AM	Armenia	FI	Finland	LT	Lithuania	SK	Slovakia
AT	Austria	FR	France	LU	Luxembourg	SN	Senegal
AU	Australia	GA	Gabon	LV	Latvia	SZ	Swaziland
AZ	Azerbaijan	GB	United Kingdom	MC	Monaco	TD	Chad
BA	Bosnia and Herzegovina	GE	Georgia	MD	Republic of Moldova	TG	Togo
BB	Barbados	GH	Ghana	MG	Madagascar	TJ	Tajikistan
BE	Belgium	GN	Guinea	MK	The former Yugoslav Republic of Macedonia	TM	Turkmenistan
BF	Burkina Faso	GR	Greece	ML	Mali	TR	Turkey
BG	Bulgaria	HU	Hungary	MN	Mongolia	TT	Trinidad and Tobago
BJ	Benin	IE	Ireland	MR	Mauritania	UA	Ukraine
BR	Brazil	IL	Israel	MW	Malawi	UG	Uganda
BY	Belarus	IS	Iceland	MX	Mexico	US	United States of America
CA	Canada	IT	Italy	NE	Niger	UZ	Uzbekistan
CF	Central African Republic	JP	Japan	NL	Netherlands	VN	Viet Nam
CG	Congo	KE	Kenya	NO	Norway	YU	Yugoslavia
CH	Switzerland	KG	Kyrgyzstan	NZ	New Zealand	ZW	Zimbabwe
CI	Côte d'Ivoire	KP	Democratic People's Republic of Korea	PL	Poland		
CM	Cameroon	KR	Republic of Korea	PT	Portugal		
CN	China	KZ	Kazakstan	RO	Romania		
CU	Cuba	LC	Saint Lucia	RU	Russian Federation		
CZ	Czech Republic	LI	Liechtenstein	SD	Sudan		
DE	Germany	LK	Sri Lanka	SE	Sweden		
DK	Denmark	LR	Liberia	SG	Singapore		
EE	Estonia						

HELICAL COMPUTED TOMOGRAPHY WITH ASYMMETRIC DETECTOR SYSTEM

Field of the Invention

The present invention relates generally to helical computed tomography scanning. More particularly, the invention relates to a method of and apparatus for reducing artifacts in tomograms generated by helical scanning with an asymmetrically arranged detector system.

Background of the Invention

Figure 1 shows an axial view of a typical third generation Computed Tomography (CT) scanner 10 that includes an X-ray source 12 and an X-ray detector system 14 secured respectively to diametrically opposite sides of an annular-shaped disk 16. The disk is rotatably mounted within a gantry support (not shown) so that during a scan, the disk continuously rotates about a Z-axis (which is normal to the plane of the page in Figure 1 and intersects the scanning plane at the mechanical center rotation of the disk, the mechanical center of rotation 18 of the disk corresponding to the "isocenter" of the reconstructed image) while X-rays pass from the source 12 through an object, such as a patient 20, positioned on a patient table 56 within the opening of the disk to the detector system 14.

The detector system 14 typically includes an array of individual detectors 22 disposed as a single row in the shape of an arc of a circle having a center of curvature at the point 24, referred to as the "focal spot", where the radiation emanates from the X-ray source 12. The X-ray source and the array of detectors are positioned so that the X-ray paths between the source and each detector all lie in a "scanning plane" that is normal to the Z-axis. Since the X-ray paths originate from what is substantially a point source and extend at different angles to the detectors, the X-ray paths form a "fan beam" 26 that is incident on the detector array 14. The X-rays incident on a single detector at a measuring instant during a scan are commonly referred to as a "ray", and each detector generates an output signal indicative of the intensity of its corresponding ray. Since each ray is

1 partially attenuated by all the mass in its path, the output signal generated by each
2 detector is representative of the density of all the mass disposed between that
3 detector and the X-ray source (i.e., the density of the mass lying in the detector's
4 corresponding ray path).

5 The output signals generated by the X-ray detectors are normally processed
6 by a signal processing portion (not shown) of the CT system. The signal
7 processing portion generally includes a data acquisition system (DAS) which filters
8 the output signals generated by the X-ray detectors to improve their signal-to-noise
9 ratio. Such a DAS is described for example in U.S. Patent No. 4,547,893. The
10 output signals generated by the DAS during a measuring interval are commonly
11 referred to as a "projection" or a "view", and the angular orientation of the disk 16
12 (and of source 12 and detector system 14 mounted on the disk 16) corresponding to
13 a particular projection is referred to as the "projection angle".

14 Figure 2 illustrates the orientation of the disk 16 (as well as the X-ray
15 source 12 and detector system 14 mounted to the disk) for generation of a fan beam
16 data point $P_r(\beta, \gamma)$ at a projection angle of β and a detector angle γ . A center line
17 40, which is used to define reference orientations, extends from the focal spot of
18 the X-ray source 12 through the Z-axis at the mechanical center of rotation 18.
19 The projection angle β is defined as the angle between a vertical axis and center
20 line 40. Each individual detector in system 14 has an associated detector angle γ
21 that is also defined with respect to center line 40. By definition, center line 40
22 intersects detector system 14 at a reference detector angle γ of 0° . A symmetric
23 detector system 14, as shown in Figure 2, extends from a detector angle of $-\gamma_m$ to
24 $+\gamma_m$. As will be discussed in greater detail below, an asymmetric detector system
25 may be said to extend from a detector angle of $-\gamma_m + \alpha$ to $+\gamma_m$. A fan beam
26 projection $P_r(\beta, \gamma)$ generated by symmetric detector system 14 includes the set of
27 data points $P_r(\beta, \gamma)$ generated by all the detectors at detector angles from $-\gamma$ to γ_m
28 for the projection angle β .

29 During a scan, the disk 16 rotates smoothly and continuously around the
30 object being scanned allowing the scanner 10 to generate a set of projections $P_r(\beta)$
31 at a corresponding set of projection angles β . In a conventional scan, the patient

1 remains at a constant Z-axis position during the scan, whereas in a helical (or
2 spiral) CT scan, the patient is translated along the Z-axis while the disk is rotated
3 about the patient (and will be described in that fashion; although, alternatively, the
4 patient can remain stationary and the disk translated along the Z-axis while being
5 rotated about the patient). Figure 3A illustrates the data collected during a
6 conventional scan, and Figure 3B illustrates the data collected during a helical scan.
7 As shown in Figure 3A, if the X-ray source 12 and detector system 14 are rotated
8 about an object 20 while the object 20 remains at a fixed Z-axis location, the
9 scanning planes associated with all the projections collected by detector system 14
10 will all lie in a common "slice plane" 50. As shown in Figure 3B, if the object 20
11 is continuously translated in the direction of the Z-axis while the disk is rotated
12 about the object 20, none of the scanning planes will be coplanar and thus lie in a
13 common slice plane. Rather, the scanning plane associated with each projection
14 will lie at a unique position along the Z-axis at a locus point on a helical set of loci.
15 Figure 3B illustrates the Z-axis coordinate of the scanning planes corresponding to
16 helical projection angles in the interval $(0, 10\pi)$. Since the value of each projection
17 depends on the Z-axis location of the patient, each projection may be considered as
18 a function of two variables, β and z .

19 Since the patient remains at a constant Z-axis position during a conventional
20 scan, this type of scanning is commonly referred to as "Constant Z-axis position
21 scanning" or CZA scanning. In helical scanning, the projections $P_i(\beta, \gamma)$ are
22 normally acquired such that z is linearly related to the view angle β so that
23 $z(\beta) = c\beta$, where c is a constant. This form of helical scanning is often referred to
24 as Constant Speed Helical (CSH) scanning.

25 Using well known algorithms, such as the inverse Radon transform, a
26 tomogram may be generated from a set of projections that all share the same
27 scanning plane, and this common scanning plane as mentioned above is referred to
28 as the "slice plane". A tomogram is representative of the density of a two
29 dimensional "slice", along the slice plane, of the object being scanned. The
30 process of generating a tomogram from the projections is commonly referred to as
31 "filtered back projection" or "reconstruction", since the tomogram may be thought

1 of as being reconstructed from the projection data. The signal processing portion
2 of a CT scanner normally includes a back projector for generating the tomograms
3 from the projections.

4 In CZA scanning, all the projections share a common scanning plane, so
5 these projections may be applied directly to the back projector for generation of a
6 tomogram. In CSH scanning, each projection has a unique scanning plane located
7 at a unique Z-axis coordinate, so CSH projections may not be applied directly to a
8 back projector. However, as is well known, the data collected during a CSH scan
9 may be interpolated in various fashions to generate a set of interpolated projections
10 that do all share a common scanning plane extending normal to the Z-axis. Each
11 interpolated projection, for example, may be generated by combining two
12 projections taken at equivalent projection angles and at different Z-axis positions.
13 These interpolated projections may be treated as CZA data and may be applied to a
14 back projector to generate a tomogram.

15 CSH scanning disadvantageously requires some form of interpolation to
16 generate a tomogram, and tomograms generated by CSH scanning therefore tend to
17 be characterized by image artifacts. Also, since the CSH scan projection data,
18 which is collected over an interval of Z-axis locations, is combined to generate the
19 interpolated CZA scan data, tomograms generated during CSH scanning have a
20 wider effective "slice plane width" than tomograms generated by CZA scanning.
21 However, CSH scanning advantageously permits rapid scanning of a large volume
22 of a patient. For example, in a time interval short enough to permit a patient to
23 comfortably hold their breath (and thereby remain relatively motionless), a CSH
24 scan may collect enough data to fully scan an entire organ such as a kidney. In
25 practice, the disk may, for example, be rotated on the order of 40π radians (i.e., 20
26 complete revolutions) during a single helical scan, and the data collected may be
27 used to generate tomograms at a plurality of slice planes.

28 A tomogram may be reconstructed from a set of fan beam projections
29 $P_f(\beta, \gamma)$ where β is in the range $(0, \beta_{\max})$. The choice of β_{\max} depends in part of the
30 desired signal-to-noise ratio of the tomogram and in part on the desired slice plane
31 width of the tomogram. Due to the rotational nature of CT scanners, the ray used

1 to measure the data point $P_f(\beta, \gamma)$ is coincident with the ray used to measure the
 2 data point $P_f(\beta + 2\pi, \gamma)$. So, in the absence of patient motion in a direction parallel
 3 to the Z-axis, projection data is periodic with period 2π , and the data point $P_f(\beta, \gamma)$
 4 equals the data point $P_f(\beta + 2\pi, \gamma)$. One method of generating a tomogram from
 5 CZA scan data uses β_{\max} equal to 2π . Since the disk 16 rotates completely around
 6 the patient, this type of scanning is often referred to as "fullscan". It is
 7 unnecessary to set β_{\max} greater than 2π , since due to the periodicity of the
 8 projection data, this will result in collecting redundant data. However, such
 9 redundant data may be collected and can be used to improve the signal-to-noise
 10 ratio of a tomogram.

11 In addition to the above-described fullscan periodicity or redundancy, CT
 12 scanners also have an associated "halfscan" redundancy that is described by the
 13 following Equation (1).

$$14 \quad P_f(\beta, \gamma) = P_f(\beta + \pi - 2\gamma, -\gamma) \quad (1)$$

16
 17 Equation (1) is true in the absence of patient motion because the ray used to
 18 measure the data point $P_f(\beta, \gamma)$ is coincident and antiparallel to the ray used to
 19 measure the data point $P_f(\beta + \pi - 2\gamma, -\gamma)$ (the rays are "antiparallel" because the
 20 relative positions of the X-ray source and detector are reversed). Known CT
 21 "halfscan" techniques use Equation (1) to permit generation of a tomogram from a
 22 set of CZA fan beam projections collected with β_{\max} equal to $\pi + 2\gamma_m$. However,
 23 such a halfscan tomogram will have a lower signal-to-noise ratio than a fullscan
 24 tomogram where β_{\max} equals 2π .

25 Helical Interpolative, or HI scanning, is a scanning method that applies the
 26 above-described fullscan technique to CSH scanning. In HI scanning, projections
 27 are acquired for β in the range of $(0, 4\pi)$ while the patient is continuously translated
 28 along the Z-axis. This data is then used to approximate a set of CZA scan data for
 29 β in the range of $(0, 2\pi)$ by linearly interpolating data on each of the opposite sides
 30 of a slice plane located at the Z-axis position corresponding to a helical projection
 31 angle of 2π . A fullscan filtered backprojection algorithm then generates a

tomogram from this approximated CZA scan data.

In HI scanning, the data point $P_f(\beta_1, \gamma_1)$, which is the data point that would result from CZA scanning at Z-axis location z_{sp} , is estimated by linear interpolation according to the following Equation (2).

$$P_f(\beta_1, \gamma_1) = w_1 P_f(\beta_1, \gamma_1) + w_2 P_f(\beta_1, \gamma_1) \quad (2)$$

where $\beta_1 = \beta_2 + 2\pi$, and $\gamma_1 = \gamma_2$. The interpolation weights w_1 and w_2 of Equation (2) are given by the following Equation (3).

$$\begin{aligned} w_1 &= \frac{\beta_2 - \beta_{sp}}{\beta_2 - \beta_1} \\ w_2 &= \frac{\beta_{sp} - \beta_1}{\beta_2 - \beta_1} \end{aligned} \quad (3)$$

One possible reconstruction method is to perform the interpolation of Equation (2) prior to filtered backprojection of the data, producing a data set with $z = z_{sp}$ and β in the interval $(0, 2\pi)$. Since filtered backprojection is linear, an alternative is to multiply the CSH scan data by interpolation weights $w(\beta, \gamma)$ and perform filtered backprojection on the entire $(0, 4\pi)$ CSH scan data set. The latter method has some computational advantages since it permits pipelining the reconstruction process and this method will be assumed for all helical algorithms subsequently presented herein. The weights $w(\beta, \gamma)$ for this method may be derived by substituting the relations $\beta_1 = \beta_2 + 2\pi$ and $\gamma_1 = \gamma_2$ into the above Equation (3) and are given by the following Equation (4).

$$w(\beta, \gamma) = \begin{cases} \frac{\beta}{2\pi} & 0 \leq \beta \leq 2\pi \\ \frac{4\pi - \beta}{2\pi} & 2\pi \leq \beta \leq 4\pi \end{cases} \quad (4)$$

The weights $w(\beta, \gamma)$ are continuous everywhere and go to zero at $\beta = 0$ and $\beta = 4\pi$, and go to unity at $\beta = 2\pi$.

1 In addition to HI scanning, other techniques are known that require 4π of
2 helical projection data to generate a tomogram, and these techniques shall be
3 referred to herein as "helical fullscan techniques". Helical fullscan techniques are
4 advantageous because they are relatively simple and straightforward to implement.
5 However, helical fullscan techniques are disadvantageous because they require 4π
6 of data to generate a single tomogram, and such tomograms are therefore
7 characterized by relatively wide slice planes.

8 Helical Halfscan, or HH, scanning is a scanning method that applies the
9 above-described halfscan techniques to CSH scanning. HH scanning
10 advantageously permits generation of a tomogram with less than 4π of projection
11 data. In HH scanning, CSH scan data is acquired for β in the range $(0, 2\pi + 4\gamma_m)$.
12 CZA scan data for β in the range $(0, \pi + 2\gamma_m)$ is approximated by linear
13 interpolation of data on opposite sides of a slice plane located at the Z-axis position
14 corresponding to a CSH scan projection angle of $\beta_{sp} = \pi + 2\gamma_m$. A known halfscan
15 filtered backprojection algorithm then generates a tomogram from this
16 approximated CZA scan data. The advantage of HH scanning over the above-
17 discussed helical fullscan techniques is that HH scanning uses fewer views, and
18 therefore less patient motion, to reconstruct each tomogram. So the effective slice
19 width of a HH scan tomogram is smaller than that of a helical fullscan tomogram.

20 Figure 4 shows the Radon space (β vs. γ) for the data used by a HH scan to
21 generate a single tomogram, and Figure 4 also illustrates the Z-axis location
22 corresponding to each projection angle β (along the vertical axis). The data shown
23 in Figure 4 is used to generate a tomogram having a slice plane, or Z-axis location,
24 corresponding to the CSH projection angle of $\beta_{sp} = \pi + 2\gamma_m$. In the absence of
25 patient translation (i.e., in a CZA scan), regions 1-4 of the Radon space as
26 illustrated in Figure 4 would provide sufficient data to reconstruct a single
27 tomogram using known halfscan techniques. Similarly, in the absence of patient
28 translation, regions 5-8 would provide sufficient data to reconstruct a single
29 tomogram. In HH, the data below the slice plane (i.e., regions 1-4) is combined
30 with the data above the slice plane (i.e., regions 5-8) to approximate CZA data for
31 regions 1-4 at the slice plane.

1 In Figure 4, regions including redundant data are similarly striped, where
 2 redundant data are defined as data that are acquired along coincident rays (either
 3 parallel or anti-parallel), and would therefore be identical in the absence of patient
 4 motion. So, regions 1, 4, and 7 are redundant; regions 2, 5, and 8 are redundant;
 5 and regions 3 and 6 are redundant. In HH, similarly striped regions are combined
 6 to approximate a set of CZA data in regions 1 through 4. Methods of combining
 7 the data are described in detail in *Computed tomography scanning with*
 8 *simultaneous patient translation*, Carl R. Crawford and Kevin F. King, Med. Phys.
 9 17 (6), Nov/Dec 1990. The reconstruction weights for HH scanning are given by
 10 the following Equation (5).

$$11 \quad w_{HH}(\beta, \gamma) = \begin{cases} 0 & 0 \leq \beta \leq 2\gamma_m - 2\gamma \\ \frac{\beta + 2\gamma - 2\gamma_m}{\pi + 2\gamma} & 2\gamma_m - 2\gamma \leq \beta \leq \pi + 2\gamma_m \\ \frac{2\pi - \beta - 2\gamma + 2\gamma_m}{\pi - 2\gamma} & \pi + 2\gamma_m \leq \beta \leq 2\pi + 2\gamma_m - 2\gamma \\ 0 & \pi + 2\gamma_m - 2\gamma \leq \beta \leq 2\pi + 4\gamma_m \end{cases} \quad (5)$$

12 Helical Extrapolative, or HE scanning, is a another scanning method that
 13 applies halfscan techniques to CSH scanning. In HE scanning, CSH scanned data
 14 is collected for β in the range of $(0, 2\pi)$. CZA scanned data for β in the range of
 15 $(0, \pi + 2\gamma_m)$ is interpolated and extrapolated from this CSH scanned data and a
 16 known halfscan technique is then used to generate a tomogram from this
 17 approximated CZA scanned data. Figure 5 illustrates the Radon space for the data
 18 used by HE scanning to generate a single tomogram at a slice plane corresponding
 19 to the CSH projection angle of $\beta_{sp} = \pi$. In the absence of patient motion (i.e., in a
 20 CZA scan), the regions 1, 2, and 3 illustrated in Figure 5 would provide sufficient
 21 data to reconstruct a single tomogram using known halfscan techniques. Similarly,
 22 in the absence of patient motion, the regions 4, 5, and 6 would also provide
 23 sufficient data to reconstruct a single tomogram. In HE scanning, the data in

regions 1-3 is combined with the data in regions 4-6 to approximate CZA data for regions 1-3 at the slice plane.

Regions 2 and 5 (as illustrated in Figure 5) are redundant, and data in these regions is interpolated to approximate CZA data for region 2. The data in regions 1 and 4 are also redundant. Since regions 1 and 4 both lie on the same side of the slice plane, the CZA scanned data for region 1 is generated by extrapolating (rather than interpolating) the CSH scanned data in regions 1 and 4. Similarly, the data in regions 3 and 6 are redundant and lie on the same side of the slice plane, so the CZA scanned data for region 3 is generated by extrapolating the CSH scan data in regions 3 and 6. The advantage of HE scanning over the above-discussed HH scanning method, is that HE scanning uses fewer views, and therefore less patient Z-axis translation, to reconstruct each tomogram. So the effective slice width of a HE scan tomogram is smaller than that of a HH scan tomogram. However, HE scanning requires some extrapolation (to generate the CZA scanned data for regions 1 and 3) whereas HH scanning relies entirely on interpolation. So to the extent that interpolation is more accurate than extrapolation, HH scan may generate more accurate tomograms.

The above-referenced article entitled *Computed tomography scanning with simultaneous patient translation* describes HE scanning in detail. The weights for the HE scanning method are given by the following Equation (6).

$$w_{HE}(\beta, \gamma) = \begin{cases} \frac{\beta+2\gamma}{\pi+2\gamma} & 0 \leq \beta \leq \pi-2\gamma \\ \frac{2\pi-\beta-2\gamma}{\pi-2\gamma} & \pi-2\gamma \leq \beta \leq 2\pi \end{cases} \quad (6)$$

The weighting function $w_{HE}(\beta, \gamma)$ is discontinuous in γ along the line $\beta = \pi - 2\gamma$, except at $\gamma = 0$ and there is an inconsistency in the discretely sampled weighted projection data leading to streaks which appear to originate from the first view and become deeper for greater distances away from the isocenter. The discontinuity can be eliminated by feathering $w_{HE}(\beta, \gamma)$ across the line $\beta = \pi - 2\gamma$.

The procedure for feathering may be understood as a general procedure for

1 smoothing a discontinuity in a function $w(x)$ at a location x_0 where $w(x)$ is given by
 2 the following Equation (7)

$$3 \quad w(x) = \begin{cases} w_1(x) & x < x_0 \\ w_2(x) & x \geq x_0 \end{cases} \quad (7)$$

4 and where $w_1(x_0) \neq w_2(x_0)$ so that $w(x)$ is discontinuous at $x=x_0$. The feathering
 5 algorithm smooths the discontinuity by extending $w_1(x)$ and $w_2(x)$ by a distance $d/2$
 6 on either side of $x=x_0$ and redefining $w(x)$ according to the following Equation (8)

$$7 \quad w(x) = \begin{cases} w_1(x) & \text{for } x \leq x_0 - \frac{d}{2} \\ w_1(x) \left[1 - f\left(\frac{x-x_0}{d} + \frac{1}{2}\right) \right] + w_2(x) f\left(\frac{x-x_0}{d} + \frac{1}{2}\right) & \text{for } x_0 - \frac{d}{2} \leq x \leq x_0 + \frac{d}{2} \\ w_2(x) & \text{for } x \geq x_0 + \frac{d}{2} \end{cases} \quad (8)$$

8 where the function $f(x)$ is equal to zero for x less than zero, and is equal to one for
 9 x greater than one, and is smooth and continuous over the interval $0 < x < 1$. An
 10 exemplary function $f(x)$ for use in the feathering algorithm is given by the
 11 following Equation (9).

$$12 \quad f(x) = \begin{cases} 0 & x < 0 \\ 3x^2 - 2x^3 & 0 \leq x \leq 1 \\ 1 & x > 1 \end{cases} \quad (9)$$

13 The above-referenced article entitled *Computed tomography scanning with*
 14 *simultaneous patient translation* reported that a feathering distance d equal to ten
 15 channels (i.e., ten times the length of a single detector) is sufficient for operation of
 16 the HE scanning method.

17 In addition to HH and HE scanning, other techniques are known for

1 generating a tomogram from less than 4π of helical projection data, and such
2 techniques shall be referred to herein as "helical halfscan techniques". Some
3 helical halfscan techniques are disclosed for example in *A General Approach to the*
4 *Reconstruction of X-ray Helical Computed Tomography*, Jiang Hsieh, Med. Phys.
5 23 (2), February 1996.

6 Figure 6 illustrates the geometry of a CT scanner having an asymmetric
7 detector system 14. This detector system includes a symmetric portion 14a
8 extending from detector angle $-\gamma_m + \alpha$ to $\gamma_m - \alpha$, and an asymmetric portion 14b
9 extending from detector angle $\gamma_m - \alpha$ to γ_m , where α is the angular extent of the
10 asymmetric portion. Detector system 14 may also be thought of as not including a
11 portion 14c extending from detector angle $-\gamma_m$ to $-\gamma_m + \alpha$. If detector system 14
12 did include the missing portion 14c, then the detector system would be symmetric.
13 A fan beam projection generated by asymmetric detector system 14 includes the set
14 of data points $P_f(\beta, \gamma)$ generated by all the detectors at detector angles from $-\gamma_m +$
15 α to γ_m .

16 Such asymmetric detector systems are often used in CT scanners so as to
17 increase the "field of view" (FOV) of the scanner without significantly increasing
18 the cost of the detector system and associated DAS. The FOV of a scanner is
19 determined by the angular extent of the detector system. For example, the FOV of
20 a scanner using the symmetric detector system illustrated in Figure 2 is equal to
21 $2\gamma_m$, and the FOV of a scanner using the asymmetric detector system illustrated in
22 Figure 6 is equal to $2\gamma_m - \alpha$. This suggests that the FOV provided by an
23 asymmetric detector system is smaller than the FOV ($2\gamma_m$) provided by a
24 comparable symmetric detector system. However, alternative symmetric and
25 asymmetric detector systems are properly compared by considering the angular
26 extent of the symmetric portion of the asymmetric detector system to be equal or
27 nearly equal to the angular extent of the alternative symmetric detector system (i.e.,
28 the $\gamma_m - \alpha$ portion of the asymmetric detector system is equal or nearly equal to γ_m
29 of the alternative symmetric detector system). So use of the asymmetric detector
30 system effectively increases the FOV of the scanner by α .

31 Another advantage of asymmetric detector systems relates to the

1 contribution that each individual detector makes to a tomogram. As is well known,
2 the importance of each detector (in terms of its contribution to tomograms)
3 decreases with increasing detector angle. So it is reasonable to eliminate half the
4 detectors having a detector angle the absolute value of which is greater than a
5 predetermined threshold. By way of example, the Anatom scanner, which is
6 manufactured by the Analogic Corporation of Peabody, Massachusetts, uses a
7 detector system that includes three hundred eighty four individual detectors. In this
8 detector system, each individual detector subtends a detector angle of 0.125° , γ_m is
9 equal to 28.843° , and α is equal to 9.687° . Although such asymmetric detector
10 systems are popular, their use complicates the process of generating helical scans.

11 The above Equation (1), which describes halfscan redundancy, is not true
12 for the asymmetric portion of the detector array, and this prevents the use of helical
13 halfscan techniques such as HH and HE scanning with asymmetric detector arrays.
14 So for prior art CT scanners including asymmetric detector arrays, helical scanning
15 may be performed using a helical fullscan technique (such as HI scanning) and data
16 collected from the entire array, or alternatively, data from the asymmetric portion
17 may be ignored and helical scanning may be performed using a helical halfscan
18 technique such as HH or HE scanning. However, it would be advantageous to be
19 able to perform helical scanning using a helical halfscan technique such as HH or
20 HE scanning and also use all the data collected by an asymmetric detector array.

21 Another problem with prior art helical scanning techniques relates to the
22 "quarter detector offset" used in many CT scanners. A CT scanner using a quarter
23 detector offset is described for example in U.S. Patent Application No.
24 08/191,428, entitled, X-RAY TOMOGRAPHY SYSTEM FOR AND METHOD
25 OF IMPROVING THE QUALITY OF A SCANNED IMAGE, filed on February
26 3, 1994, (Attorney Docket No. ANA-044). In general, in a CT scanner using a
27 quarter detector offset, the center line 40 (as shown in Figure 2), which passes
28 through the focal spot of the X-ray source 12 and the Z-axis, does not intersect the
29 center of one of the detectors in the detector system 14. Rather, it intersects one of
30 the detectors, which shall be referred to herein as the "central detector", at a
31 location slightly offset from the central detector's center. This insures that the ray

1 measured by the central detector at a projection angle β is not coincident with the
2 ray measured by that detector at a projection angle of $\beta + \pi$. Rather, the two rays
3 are offset from one another. As is well known, using such a quarter detector offset
4 increases the amount of data (by increasing the number of unique sampling points)
5 collected by a scanner during a 360° rotation of the disk. However, use of a
6 quarter detector offset complicates the process of CSH scanning, regardless of
7 whether the detector system used is symmetric or asymmetric.

8 As is well known, the fan beam projection data collected during a CT scan
9 is often "rebinned" or "reordered" to form reordered projection data, such that all
10 the rays used to generate a single reordered projection are mutually parallel. In
11 systems using a quarter detector offset, the reordered projections are typically
12 "interleaved" to generate parallel beam projection data. Figure 7A illustrates some
13 of the individual rays in a fan beam projection 100 taken at a fan beam projection
14 angle of zero degrees, and Figure 7B illustrates some of the individual rays in a
15 parallel beam projection 102 taken at a parallel beam projection angle of zero
16 degrees. As shown, none of the rays in the fan beam projection 100 are parallel to
17 one another, while all of the rays in the parallel beam projection 102 are mutually
18 parallel. Since all of the rays emanate from the focal spot of the X-ray source 12 to
19 form a fan beam, the CT scanner may not generate all the rays of a parallel beam
20 projection simultaneously. However as is well known, the fan beam projection
21 data may be reordered and interleaved to generate parallel beam projections.
22 Known fullscan and halfscan parallel beam reconstruction algorithms may generate
23 a tomogram from CZA parallel beam projections $P_p(\beta, \gamma)$ for β in the range $(0, 2\pi)$
24 and $(0, \pi)$, respectively.

25 Figures 8A and 8B illustrate a method of generating the reordered
26 projections. Figures 8A and 8B show the positions of X-ray source 12 and detector
27 system 14 during generation of two successive fan beam projections. Figures 8A
28 and 8B show detector system 14 as including seven individual detectors, 22:1,
29 22:2, 22:3, 22:4, 22:5, 22:6, and 22:7. Most detector systems include hundreds of
30 detectors, and as stated above, the detector system used in the Anatom scanner
31 includes three hundred eighty four detectors. However, for convenience of

1 illustration, the seven detector system shall now be discussed. During a scan, as
2 shown in Figures 8A and 8B, X-ray source 12 and detector system 14 rotate in a
3 counter clockwise direction about the Z-axis, the latter extending perpendicular to
4 the sheet of the drawing. During the first projection, shown in Figure 8A, a ray
5 114 is incident on a detector 22:4 (i.e., the detector in the fourth channel of
6 detector system 14). During the next projection, shown in Figure 8B, a ray 116 is
7 incident on detector 22:3 (i.e., the detector in the third channel of detector system
8 14). When the spacing between the individual detectors is matched to the amount
9 of disk rotation between generation of successive fan beam projections, the ray 114
10 is parallel to, and slightly offset from, ray 116. When this basic relationship is true
11 for all detectors and all fan beam projections, any two rays incident on adjacent
12 detectors during successive fan beam projections are parallel and are offset from
13 each other. As was stated above, in the Anatom scanner, the individual detectors
14 are spaced apart by 0.125° , and consequently, in that scanner, successive
15 projections are separated by a projection angle that is also equal to 0.125° . This
16 allows the fan beam data collected by that scanner to be reordered into reordered
17 projections.

18 When a symmetric detector system 14 includes a quarter detector offset, the
19 reordered parallel beam projections may then be interleaved to generate interleaved
20 parallel beam projections. Each interleaved parallel beam projection is generated
21 by combining the data from two reordered projections taken at reordered projection
22 angles that are 180° apart to form a single denser projection. Figures 9A and 9B
23 illustrate the spatial relationship between X-ray source 12, a cross section of patient
24 20, and symmetric detector system 14 for projection angles of zero and 180°
25 degrees, respectively. In Figures 9A and 9B, symmetric detector system 14 is once
26 again shown for convenience of illustration as containing seven individual
27 detectors. The illustrated detector system 14 has a quarter detector offset so that
28 the center liner 40 which extends from the focal spot of the X-ray source 12
29 through the Z-axis does not intersect the center of the central detector 22:4.
30 Rather, the center line 40 intersects the central detector 22:4 at a point that is offset
31 from the center by one quarter of the detector's width.

1 Figure 10 illustrates the spatial relationship between symmetric detector
2 system 14 at projection angles of zero and 180 degrees, and the rays 120, 122, 124
3 incident on three of the detectors. Because of the quarter detector offset between
4 symmetric detector system 14 and center line 40, the detector system 14 at a
5 projection angle of zero degrees is offset from the detector system 14 at 180
6 degrees. Consequently, the ray 120 that is incident on the sixth channel detector
7 22:6 for a projection angle of 180 degrees falls precisely between the rays 122 and
8 124 that are incident on detectors 22:2 and 22:3, respectively, for a projection
9 angle of zero degrees. The interleaved set of data provided by the detector system
10 at 180 degrees is thus displaced by one-half a detector width relative to the set of
11 data provided by the detector system at zero degrees. In this example, detector
12 22:6 may be thought of as a "center" detector and detectors 22:2 and 22:3 may be
13 thought of as "opposite-adjacent" detectors. At each projection angle, each
14 detector measures the integral of the density of mass along a particular ray path,
15 and in general, the ray paths used by the opposite-adjacent detectors are closer to
16 the ray path used by the center detector than are the ray paths used by any other
17 detectors (e.g., the ray path used by detectors 22:2, 22:3 at a projection angle of
18 zero degrees are closer to the ray path used by detector 22:6 at a projection angle
19 of 180 degrees than are the ray paths used by detectors 22:5, 22:7 at a projection
20 angle of 180 degrees). Any two reordered projections separated by 180 degrees
21 may be interleaved using this relationship between center and opposite-adjacent
22 detectors to form a single denser parallel beam projection.

23 A single interleaved parallel beam projection generated by a symmetric
24 detector system may be represented as a set of data points D:1, D:2, D:3, . . . ,
25 D:N. In this representation, all of the odd data points (e.g., D:1 and D:3) are
26 contributed by a reordered projection taken at a reordered projection angle of β ,
27 and all of the even data points (e.g., D:2 and D:4) are contributed by a reordered
28 projection taken at a reordered projection angle of $\beta + \pi$.

29 Two reordered projections generated at reordered projection angles of β and
30 $\beta + \pi$ by an asymmetric detector system 14 (such as the one shown in Figure 6)
31 may also be interleaved to generate a single interleaved parallel beam projection.

1 However, the procedure for interleaving data collected by an asymmetric detector
 2 system is different from the procedure used for data collected by a symmetric
 3 detector system. This is so because the data required for interleaving the
 4 asymmetric portion 14b could only be collected by the missing portion 14c shown
 5 in Figure 6. So when an asymmetric detector system 14 is used, the resulting
 6 interleaved parallel beam projections include a central region and two exterior
 7 regions. In the central region, the data points are structured identically to
 8 projections generated by symmetric detector systems and every other data point is
 9 contributed by a different reordered projection. In one of the exterior regions, all
 10 of the data points are contributed by the reordered projection generated at a
 11 reordered projection angle of β , and in the other exterior region, all of the data
 12 points are contributed by the reordered projection generated at a reordered
 13 projection angle of $\beta + \pi$. Since the data points in the exterior regions are not
 14 interleaved, the angular spacing between adjacent data points in the exterior regions
 15 is double the angular spacing between adjacent data points in the central region.

16 A single interleaved parallel beam projection generated by an asymmetric
 17 detector system may be represented as a set of data points $D:i$ for all integers i
 18 from one to N_m , where N_m equals $2N_s$ plus $2N_a$, where N_s equals the number of
 19 detectors in the symmetric portion 14a of the detector system, and where N_a equals
 20 the number of detectors in the asymmetric portion 14b of the detector system. In
 21 this representation, all the data points $D:i$ are undefined for $i=2j+1$ and for
 22 $i=N_m-2j$ for all integers j greater than or equal to zero and less than or equal to N_a
 23 - 1. These undefined data points are the odd data points in one of the exterior
 24 regions and the even data points in the other exterior region. These undefined data
 25 points could have only been collected by the missing portion 14c of the detector
 26 system. In this representation, all of the (defined) odd data points are contributed
 27 by a reordered projection generated at a reordered projection angle of β and all of
 28 the (defined) even data points are contributed by reordered projection generated at
 29 a reordered projection angle of $\beta + \pi$.

30 Hereinafter, parallel beam projections taken at a parallel beam projection
 31 angle of β shall be referred to as including a set of "odd data points" and a set of

1 "even data points", and the term "odd data points" shall refer to data points
2 measured at a reordered projection angle β , and the term "even data points" shall
3 refer to data points measured at a reordered projection angle of $\beta + \pi$. Further, the
4 term "odd data points" shall also refer to the data points in the fan beam projections
5 that may be reordered and interleaved to form the odd data points of a parallel
6 beam projection, and the term "even data points" shall also refer to the data points
7 in the fan beam projections that may be reordered and interleaved to form the even
8 data points of a parallel beam projection.

9 In the central region of an interleaved parallel beam projection, the ray path
10 used to generate the i th data point $D:i$ is closer to the ray paths used to generate the
11 adjacent data points $D:i-1$ and $D:i+1$ than to any other ray paths. However, the
12 difference between the measurement times of adjacent data points (e.g., $D:i$ and
13 $D:i-1$) is much greater than the difference between the measurement times of
14 alternate data points (e.g., $D:i$ and $D:i-2$). For example, if $T:i$ represents the time
15 that a data point $D:i$ is measured, then $T:i$ minus $T:i-1$ is much greater than $T:i$
16 minus $T:i-2$. This is true because all of the even points of a single parallel beam
17 projection are contributed by a single reordered projection (and all the data points
18 of a reordered projection are generated by a set of adjacent fan beam projections),
19 however, adjacent data points in the central region of a parallel beam projection are
20 contributed by two different reordered projections generated approximately 180°
21 apart from one another. So the measurement times of such adjacent data points are
22 separated by the time required for the disk to rotate approximately 180° .

23 In the absence of patient translation motion (i.e., in a CZA scan during
24 which the patient is not moved) the portions of the patient measured by adjacent
25 data points of the central region of a parallel beam projection are physically
26 proximal to one another. However, in the central region of a parallel beam
27 projection generated from CSH scan data, the portions of the patient measured by
28 adjacent data points are axially separated by a relatively large distance because the
29 patient is translated a considerable distance in the direction of the Z-axis during the
30 time required for the disk to rotate approximately 180° . This leads to a
31 discrepancy between the even data points and the odd data points in every single

1 parallel beam projection generated during a CSH scan. Further, there is an even
2 larger discrepancy in the helical weights applied to even and odd data points.
3 These discrepancies appear as high frequency noise in the projection data and
4 complicate the process of generating tomograms from CSH data collected with
5 offset detector systems.

6 In particular, this high frequency noise complicates the process of
7 performing "isocenter interpolation" and also complicates the process of
8 suppressing streak artifacts from tomograms generated from CSH scans. As is well
9 known, isocenter interpolation refers to an interpolation process used to equalize
10 the linear spacing between data points in a parallel beam projection. Prior art
11 techniques of performing isocenter interpolation, and/or streak suppression do not
12 function well when applied to CSH scan data, and tend to generate tomograms that
13 are characterized by a relatively large amount of image artifacts. One prior art
14 method of reducing these artifacts is to select a convolution kernel for filtered
15 backprojection that includes a low pass filter for suppressing the high frequency
16 information caused by the quarter detector offset. While such a convolution kernel
17 effectively suppresses some artifacts, it also has the unwanted consequence of
18 reducing the resolution of the resulting tomogram.

19

20 **Objects of the Invention**

21 It is an object of the present invention to substantially reduce or overcome
22 the above-identified problems of the prior art.

23 Another object of the present invention is to provide an improved method of
24 and apparatus for helical scanning that can generate a tomogram from all the data
25 collected by an asymmetric detector system using a helical halfscan technique.

26 And another object of the present invention is to provide an improved
27 method and apparatus for helical scanning that can generate a tomogram that has a
28 reduced slice plane width from all of the data collected by an asymmetric detector
29 array.

30 Still another object of the present invention is to provide an improved
31 method of and apparatus for helical scanning for use with asymmetric detector

1 arrays that use a detector offset.

2 And still another object of the present invention is to provide an improved
3 method of and apparatus for performing isocenter interpolation for data collected
4 during a helical scan.

5 And yet another object of the present invention is to provide an improved
6 method of and apparatus for performing streak artifact suppression for data
7 collected during a helical scan.

8 9 **Summary of the Invention**

10 These and other objects are provided by an improved helical weighting
11 system that applies a helical halfscan technique to data collected by a symmetric
12 portion of an asymmetric detector system and applies a helical fullscan technique to
13 data collected by an asymmetric portion of the asymmetric detector system. These
14 objects are further provided by an equi-angle interpolator, a streak artifact
15 suppression filter, and an isocenter interpolator that preserve the distinction
16 between even and odd data points in parallel beam projection data.

17 Still other objects and advantages of the present invention will become
18 readily apparent to those skilled in the art from the following detailed description
19 wherein several embodiments are shown and described, simply by way of
20 illustration of the best mode of the invention. As will be realized, the invention is
21 capable of other and different embodiments, and its several details are capable of
22 modifications in various respects, all without departing from the invention.
23 Accordingly, the drawings and description are to be regarded as illustrative in
24 nature, and not in a restrictive or limiting sense, with the scope of the application
25 being indicated in the claims.

26 27 **Brief Description of the Drawings**

28 For a fuller understanding of the nature and objects of the present invention,
29 reference should be had to the following detailed description taken in connection
30 with the accompanying drawings in which the same reference numerals are used to
31 indicate the same or similar parts wherein:

1 Figure 1 shows an axial view of a prior art CT scanner;

2 Figure 2 is a simplified schematic, axial view of the CT scanner shown in
3 Figure 1 showing the orientations of the disk, X-ray source, and detector system
4 for generation of a projection at a projection angle of β ;

5 Figure 3A illustrates an isometric view of the slice plane of data collected
6 during a CZA scan;

7 Figure 3B illustrates an isometric view of a set of loci of the Z-axis position
8 of every fan beam projection generated during a CSH scan for fan beam projections
9 in the range $(0, 10\pi)$;

10 Figure 4 is a graph of the Radon space used by a HH scan to generate a
11 tomogram at a slice plane corresponding to a fan beam projection angle of $\pi + 2\gamma_m$;

12 Figure 5 is a graph of the Radon space used by a HE scan to generate a
13 tomogram at a slice plane corresponding to a fan beam projection angle of π ;

14 Figure 6 is a simplified schematic, axial view of a CT scanner having an
15 asymmetric detector system;

16 Figure 7A is a simplified schematic, axial view of a prior art CT scanner
17 illustrating some of the rays that form a single fan beam projection;

18 Figure 7B is a simplified schematic, axial view of a prior art CT scanner
19 illustrating some of the rays of a single parallel beam projection;

20 Figures 8A and 8B illustrate one method of rebinning fan beam projection
21 data into reordered projection data;

22 Figures 9A and 9B show simplified schematic, axial views of a prior art
23 detector system at projection angles of 0° and 180° , respectively;

24 Figure 10 shows the spatial relationship between the detector system of
25 Figures 9A and 9B at projection angles of 0° and 180° ;

26 Figure 11 is a graph of the Radon space used by a "Helical Asymmetric"
27 (HA) scan according to the invention to generate a tomogram at a slice plane
28 corresponding to a projection angle of 2π ;

29 Figure 12 is a graph of the Radon space used by HA according to the
30 invention to generate a tomogram at a slice plane corresponding to a projection
31 angle of $2\pi - \phi$;

1 Figure 13A illustrates a simplified schematic view of a portion of a
2 projection collected by an asymmetric portion of a detector system;

3 Figure 13B illustrates a simplified schematic view of portions of a
4 projection collected by an asymmetric portion of a detector system as well as a
5 portion of a projection that could be collected by a missing portion of a detector
6 system if such missing portion were present;

7 Figure 14 shows a block diagram of a portion of one preferred CT scanner
8 constructed according to the invention for use with asymmetric detector systems;

9 Figure 15 shows the uneven linear spacing in a parallel beam projection and
10 the even spacing in projection generated by an isocenter interpolator;

11 Figure 16 shows a block diagram of a portion of another preferred CT
12 scanner constructed according to the invention for use with asymmetric detector
13 systems having a quarter detector offset; and

14 Figure 17 shows a block diagram of a streak artifact suppression filter
15 constructed according to the invention for use with CSH scanning.

16 17 Detailed Description of the Drawings

18 The present invention provides improved methods and apparatus for
19 generating tomograms from data collected during CSH scans. One improved
20 method provided by the present invention is referred to herein as "Helical
21 Asymmetric", or HA scanning. HA scanning assumes that an asymmetric detector
22 array (e.g., such as the one shown in Figure 6) is used to collect the projection
23 data. In HA scanning, CSH data $P_r(\beta, \gamma)$ is acquired for β in the range $(0, 4\pi)$ and
24 for γ in the range $(-\gamma_m + \alpha, \gamma_m)$. HA scanning uses a helical fullscan technique
25 (such as HI or some other helical fullscan technique) to process the CSH scan data
26 collected by the asymmetric portion of the detector array, and uses a helical
27 halfscan technique (such as HH scan, HE scan, or some other helical halfscan
28 technique) to process the CSH scan data collected by the symmetric portion of the
29 detector array. More specifically, HA scanning uses a helical fullscan technique to
30 process the fan beam projection data points $P_r(\beta, \gamma)$ for γ in the range $(\gamma_m - \alpha, \gamma_m)$
31 (i.e., the asymmetric portion) and β in the range $(0, 4\pi)$ so as to approximate CZA

1 scan data for β in the range $(0, 2\pi)$ and γ in the range $(\gamma_m - \alpha, \gamma_m)$. HA scanning
2 also uses a helical halfscan technique to process the fan beam projection data points
3 $P_f(\beta, \gamma)$ for γ in the range $(-\gamma_m + \alpha, \gamma_m - \alpha)$ (i.e., the symmetric portion) and β in the
4 range $(2\pi - \psi/2, 2\pi + \psi/2)$ (where ψ is the extent of fan beam projections required
5 for a halfscan helical technique, e.g., ψ equals $2\pi + 4\gamma_m$ for a HH scan and equals
6 2π for a HE scan) so as to approximate CZA scanned data for β in the range
7 $(2\pi - \psi/2, 2\pi)$ and γ in the range $(-\gamma_m + \alpha, \gamma_m - \alpha)$. HA scanning then uses the two
8 sets of approximated CZA scanned data (i.e., one set generated from data collected
9 by the asymmetric portion of the detector system, and another set generated from
10 data collected by the symmetric portion of the detector system) to generate a single
11 tomogram at a slice plane corresponding to the CSH projection angle of 2π .

12 As those skilled in the art will appreciate, a tomogram may be generated
13 from the data collected by the symmetric portion of the detector system using a
14 helical halfscan technique. Similarly, another tomogram may also be generated
15 from the data collected by the asymmetric portion of the detector system using a
16 helical fullscan technique. The signal-to-noise ratio of these tomograms will in
17 effect be limited because each tomogram is generated using only data collected by a
18 limited portion of the detector system. HA scanning advantageously uses these two
19 portions of data (i.e., the portions generated by the symmetric and asymmetric
20 portions of the detector system) to generate a single tomogram having an improved
21 signal-to-noise ratio. Since a helical halfscan technique is applied to the data
22 collected by the symmetric portion of the detector system, the portion of the
23 tomogram generated from this data has an associated slice plane width that is
24 determined by the helical halfscan technique. Similarly, since a helical fullscan
25 technique is applied to the data collected by the asymmetric portion of the detector
26 system, the portion of the tomogram that is generated from this data has an
27 associated slice plane width that is determined by the helical fullscan technique.
28 So, HA scanning (1) advantageously minimizes the slice plane width of at least a
29 portion of the tomogram, (2) advantageously permits reconstruction of a tomogram
30 using all of the data collected by an asymmetric detector system, and (3) improves
31 the signal-to-noise ratio of the reconstructed tomograms.

1 Figure 11 illustrates the Radon space for data used by a HA scan. When
 2 the data illustrated in Figure 11 is collected with an asymmetric detector system of
 3 the type shown in Figure 6, regions 2, 4, and 5 represent the data collected by the
 4 symmetric portion 14a of the detector system. Region 3 represents data collected
 5 by the asymmetric portion 14b of the detector system. Finally, region 1 represents
 6 data that would be collected by the missing portion 14c of the detector system, if
 7 such a portion were present. In a HA scan, a helical halfscan technique (e.g., a
 8 HH scan or HE scan) is applied to the data collected by the symmetric portion of
 9 the detector system (i.e., regions 2, 4, and 5), and a helical fullscan technique
 10 (e.g., HI scan) is applied to the data collected by the asymmetric portion of the
 11 detector system (i.e., region 3). Since the helical halfscan technique only requires
 12 CSH fan beam projection data with β in the range $(2\pi - \psi/2, 2\pi + \psi/2)$, the data in
 13 region 2 is sufficient to generate a tomogram, and the data in regions 4 and 5 may
 14 be discarded. Discarding the data in regions 4 and 5 effectively reduces the slice
 15 plane width of the part of the tomogram that is generated by the symmetric portion
 16 of the detector array.

17 One method of implementing a HA scan is to multiply the data in the Radon
 18 space (as illustrated in Figure 11) by a set of weights prior to performing a filtered
 19 backprojection. The weights for region 1 are zero, since region 1 represents data
 20 that is not actually collected by the asymmetric detector system. The weights for
 21 regions 4 and 5 are also zero, since the data in these regions are preferably
 22 discarded so as to reduce the slice plane width for at least a portion of the
 23 tomogram. The weights for region 2 are determined by the helical halfscan
 24 technique and the weights for region 3 are determined by the helical fullscan
 25 technique. When scanning technique HI is used as the helical fullscan technique,
 26 the weights for region 3 are given by the above-listed Equation (4), and when a HH
 27 or HE scanning technique is used for the helical halfscan technique, the weights for
 28 region 2 are determined in part by the above-listed Equations (5) or (6),
 29 respectively. Equations (5) and (6) describe the weights $w_{HH}(\beta, \gamma)$ and $w_{HE}(\beta, \gamma)$,
 30 for a HH and HE scanning techniques, respectively, for β in the interval $(0, \psi)$.
 31 However, in region 2, β extends over the interval $(2\pi - \psi/2, 2\pi + \psi/2)$. The weights

1 may therefore be adapted for use with region 3 by offsetting β so that the HH and
 2 HE weights for use with region 2 data are given by $w_{HH}(\beta - \psi/2, \gamma)$ and
 3 $w_{HE}(\beta - \psi/2, \gamma)$, respectively.

4 One potential problem with a HA scan is that the weights applied to the
 5 Radon space, as illustrated in Figure 11, are discontinuous along the vertical lines
 6 $\gamma = -\gamma_m + \alpha$ and $\gamma = \gamma_m - \alpha$. These discontinuities in the weights can lead to streaks
 7 originating from off-center objects in the tomogram. The streaks can be eliminated
 8 by feathering the halfscan weights (i.e., the weights applied to region 2 data) with
 9 the fullscan weights (i.e., the weights applied to region 3 data) and with the zero
 10 weights (i.e., the weights relating to region 1) along these two lines of
 11 discontinuity. Preferably, the feathering is performed in the regions where
 12 $-\gamma_m + \alpha < \gamma < -\gamma_m + \alpha + \zeta$ and where $\gamma_m - \alpha - \zeta < \gamma < \gamma_m - \alpha$, where ζ represents the
 13 angular extent of the feathering region. The boundaries of the feathering region are
 14 shown as vertical lines in Figure 11 located where $\gamma = -\gamma_m + \alpha$, where
 15 $\gamma = -\gamma_m + \alpha + \zeta$, where $\gamma = \gamma_m - \alpha - \zeta$, and where $\gamma = \gamma_m - \alpha$. The feathering may be
 16 performed as discussed above in connection with the above-listed Equation (8). In
 17 one preferred embodiment, ζ is selected so that the feathering region extends over a
 18 region of about twenty detectors.

19 As stated above, the disk (and X-ray source and detector system) may rotate
 20 on the order of, for example, twenty complete revolutions (i.e., 40π) about the
 21 patient during a single CSH scan. The data collected during this scan may be used
 22 to generate a plurality of tomograms at a corresponding plurality of slice planes.
 23 As thus far described, HA scanning requires fan beam projection data for β in the
 24 range $(x, x + 4\pi)$, where x is an arbitrary starting angle, to generate a tomogram at a
 25 slice plane corresponding to a projection angle of $x + 2\pi$. Referring to Figure 3B
 26 (which illustrates the Z-axis position corresponding to each projection angle in a
 27 helical scan for projection angles in the interval $(0, 10\pi)$), as thus far described, HA
 28 scanning may be used to generate a tomogram at any slice plane (i.e., Z-axis
 29 position) corresponding to projection angles in the range $(2\pi, 8\pi)$. However, as
 30 thus far described, HA scanning can not be used to generate any tomograms at slice
 31 planes corresponding to projection angles in the range $(0, 2\pi)$ (i.e., at the beginning

of the scan), and in the range $(8\pi, 10\pi)$ (i.e., at the end of the scan).

Still referring to Figure 3B, a HA scan can be modified to generate tomograms at slice planes corresponding to projection angles in the range $(\pi, 2\pi)$ (i.e., at the beginning of the scan) and in the range $(8\pi, 9\pi)$ (i.e., at the end of the scan). Figure 12 illustrates a modified version of the Radon space which may be used to generate tomograms at slice planes corresponding to projection angles in the range $(\pi, 2\pi)$. As compared with Figure 11, in Figure 12 region 2 has been shifted downward by an amount ϕ , thus shrinking the extent of region 5 and expanding the extent of region 4. However, since region 2 still extends over a range of ψ projection angles, a helical halfscan technique may be used to reconstruct a tomogram at a slice plane corresponding to a projection angle of $2\pi - \phi$ from the data in region 2. Similarly, the 4π of projection data in region 3 may also be used to contribute to that tomogram. The weights applied to regions 2 and 3 should also be offset to an amount equal to ϕ . So, if HH or HE scanning techniques are used for the helical halfscan technique, the weights for region 2 are given by $w_{HH}(\beta - \pi - 2\gamma_m + \phi, \gamma)$ or $w_{HE}(\beta - \pi + \phi, \gamma)$, respectively. Similarly, if a HI scanning technique is used for the helical fullscan technique, the weights for region 3 are given by the following Equation (10).

$$w_{HI}(\beta, \gamma) = \begin{cases} \frac{\beta + \phi}{2\pi} & \beta \leq 2\pi \\ \frac{4\pi - \beta - \phi}{2\pi} & \text{elsewhere} \end{cases} \quad (10)$$

Selecting ϕ equal to π permits reconstruction of a tomogram at a slice plane corresponding to a projection angle of π . So this procedure may be used at the beginning of the scan to generate tomograms at slice planes corresponding to projection angles in the interval $(\pi, 2\pi)$. Those skilled in the art will appreciate that a similar procedure (involving raising region 2 of the Radon space rather than lowering it) may be used to generate tomograms at the end of a scan.

Thus far, the invention has been discussed in connection with filtered backprojection algorithms that generate tomograms from fan beam projection data.

While a HA scan has been discussed in connection with fan beam CT systems,

1 those skilled in the art will appreciate that HA scanning may also be used with
2 parallel beam CT systems. The operation of a HA scan may be intuitively
3 understood in terms of a parallel beam reconstruction algorithm. The data in
4 region 2 of Figure 11 may be rebinned and interleaved to generate CZA parallel
5 beam projections $P_p(\beta, \gamma)$ for β in the range $(0, \pi)$ and the data in region 3 of Figure
6 11 may be rebinned and interleaved to generate CZA parallel beam projections
7 $P_p(\beta, \gamma)$ for β in the range $(0, 2\pi)$. Initially it may appear that a factor of two is
8 missing from one of the two sets of weights. However, fan beam data are not
9 collected for region 1 and the doubled set of data in region 3 are used to
10 compensate for the missing data in region 1. Figures 13A and 13B illustrate this
11 relationship.

12 Figure 13A shows the ray paths R1 for the portion of a parallel beam
13 projection that is measured by the asymmetric portion 14b of detector system 14.
14 In addition to the ray paths R1, Figure 13B shows the rays paths R2 for the portion
15 of a parallel beam projection that could have been measured by the missing portion
16 14c of the detector system if such a missing portion were present. As those skilled
17 in the art will appreciate, in the absence of patient translation motion, the data
18 collected by the asymmetric portion 14b for parallel beam projection angles in the
19 range $(0, 2\pi)$ is equivalent to the data that would be collected by detector portions
20 14b, 14c for parallel beam projection angles in the range $(0, \pi)$. So the extra π of
21 projection data collected for the asymmetric portion 14b compensates for the data
22 that is not collected by the missing portion 14c.

23 When HA scanning is used in connection with a parallel beam filtered back
24 projection algorithm, the weights may be applied to the Radon space (as illustrated
25 in Figure 11) before or after rebinning and/or interleaving. When the weights are
26 applied prior to rebinning, the weights are preferably feathered between regions 2
27 and 4 near the horizontal line where β equals $2\pi + \psi/2$ and between regions 2 and 5
28 near the horizontal line where β equals $2\pi - \psi/2$. This feathering is analogous to the
29 well known overscan procedures used in CZA scanning. Overscan compensates
30 for patient translation motion that occurs during a CZA scan and causes the
31 projection data at the starting projection angle to be different than the projection

1 data at the finishing angle (e.g., where the finishing angle equals the starting angle
2 plus 2π). Overscan is described, for example, in detail in D.L. Parker, V. Smith,
3 and J.H. Stanley, *Dose minimization in computed tomography overscanning*,
4 Medical Physics, Vol. 8, 706-711 (1981).

5 Figure 14 shows a block diagram of a portion of one preferred CT scanner
6 200 constructed according to the invention for generating tomograms from CSH
7 scan data. Scanner 200 includes asymmetric detector system 14, a helical
8 weighting system 210, a parallel beam converter 212, a prior art equi-angle
9 interpolator 214, a prior art isocenter interpolator 216, and a back projector 220.
10 Asymmetric detector system 14 collects the fan beam projection data and applies it
11 to helical weighting system 210. The latter applies the feathered weights for the
12 HA scan to the fan beam projection data as has been discussed above in connection
13 with Figures 11 and 12. The weighted projection data is then applied to parallel
14 beam converter 212 which reorders and interleaves the fan beam projection data to
15 generate parallel beam projection data. Equi-angle interpolator 214 receives the
16 parallel beam projections and generates therefrom equi-angle projections by filling
17 in the undefined data points in the exterior regions of the parallel beam projections.
18 Isocenter interpolator 216 receives the equi-angle projections and generates
19 therefrom isocenter projections. Back projector 220 receives the isocenter
20 projections and generates a tomogram from this data using a parallel beam
21 reconstruction algorithm. In an alternative embodiment of scanner 200, parallel
22 beam converter 212, equi-angle interpolator 214, and isocenter interpolator 216 are
23 eliminated, and back projector 214 generates tomograms using a fan beam
24 reconstruction algorithm.

25 Since scanner 200 includes an asymmetric detector system, every parallel
26 beam projection generated by converter 212 includes a central region and two
27 exterior regions. Further, as previously described, every other data point in the
28 exterior regions is undefined. Equi-angle interpolator 214 generates the equi-angle
29 projections from the parallel beam projections by replacing every undefined data
30 point in the parallel beam projections with an interpolated point. As is known in
31 the prior art, interpolator 214 may generate these interpolated data points according

1 to weighted averages of neighboring data points. For example, interpolator 214
 2 may generate a value for an undefined data point D:i according to a weighted
 3 average of defined adjacent data points D:i-1 and D:i+1. By replacing the
 4 undefined data points with interpolated data points, interpolator 214 insures that the
 5 angular spacing between all adjacent data points in the equi-angle projections are
 6 equal.

7 Isocenter interpolator 216 generates the isocenter projections from the equi-
 8 angle projections so that the linear distance between all adjacent data points in the
 9 isocenter projections are all equal. Figure 15 shows an equi-angle projection 250
 10 including data points D:i, for all i from one to seventeen. Since projection 250 is
 11 an equi-angle projection, all the data points D:i are defined. Most equi-angle
 12 projections include hundreds of data points, however, for convenience of
 13 illustration, the seventeen data point projection 250 will now be discussed. Figure
 14 15 illustrates the linear spacing between each data point D:i (i.e., the linear spacing
 15 between the rays used to generate the data points) in projection 250. As shown, the
 16 spacing between data points near the center of the projection 250 is much greater
 17 than the spacing between the data points near the ends of the projection. This
 18 uneven spacing is a well known consequence of converting fan beam projections to
 19 parallel beam projections. Isocenter interpolator 216 generates an isocenter
 20 projection 260 of data points C:i from the equi-angle projection 250. As shown, all
 21 the data points in projection 260 are equally spaced apart from one another. As is
 22 known in the prior art, isocenter interpolator 216 may generate each data point C:i
 23 according to a weighted average of a neighborhood of data points in projection 250
 24 according to the following Equation (11).

$$25 \quad C:i = \sum_{j=-x/2}^{x/2} b:j * D:j \quad (11)$$

26 Back projector 220 then generates a tomogram from the isocenter
 27 projections. The operation of helical weighting system 210 permits scanner 200 to
 28 generate improved tomograms. Scanner 200 functions well when asymmetric
 29 detector system 14 does not use a detector offset (e.g., quarter detector offset).

1 However, the invention also provides methods of and apparatus for generating
2 tomograms from CSH scan data collected with asymmetric detector systems that do
3 use a detector offset. Figure 16 shows a block diagram of a preferred scanner 300
4 constructed according to the invention for generating tomograms from CSH scan
5 data collected with an asymmetric detector system that includes a quarter detector
6 offset. Improved scanner 300 includes asymmetric offset detector system 14,
7 helical weighting system 210, parallel beam converter 212, an improved helical
8 equi-angle interpolator 314, an improved helical streak suppression filter 318, an
9 improved helical isocenter interpolator 316, and back projector 220.

10 In scanner 300, the asymmetric offset detector system 14 collects fan beam
11 projection data and applies this data to helical weighting system 210. The latter
12 applies the feathered weights for HA to the fan beam data and then applies the
13 weighted fan beam projection data to parallel beam converter 212. Converter 212
14 reorders and interleaves the fan beam data to generate parallel beam projections,
15 each of which is characterized by a central region and two exterior regions.
16 Improved equi-angle interpolator 316 generates equi-angle projections by doubling
17 the value of all data points in the exterior regions and by replacing all undefined
18 data points with data points having a value of zero. The equi-angle projections
19 generated by interpolator 314 are applied to streak suppression filter 318 which
20 suppresses high amplitude, high spatial frequency components in the projection
21 data so as to suppress streaks in the resulting tomograms. The filtered projections
22 generated by streak suppression filter 318 are applied to improved isocenter
23 interpolator 316 which generates isocenter projections. Back projector 214
24 receives the isocenter projections generated by isocenter interpolator 316 and
25 generates tomograms from this data.

26 In scanner 300, the parallel beam projections generated by converter 212
27 are applied to improved helical equi-angle interpolator 314. In the prior art, equi-
28 angle interpolation is normally performed by interpolating a new data point
29 between every pair of adjacent data points in each of the exterior regions.
30 However, rather than perform the prior art equi-angle interpolation, improved
31 equi-angle interpolator 314 replaces the undefined data points with data points that

1 have a value of zero and doubles the value of all the data points in the exterior
2 regions. Prior art methods of equi-angle interpolation essentially use the even data
3 points in one exterior region to generate an interpolated set of odd data points for
4 that region, and also use the odd data points in the other exterior region to generate
5 an interpolated set of even data points for that region. Further, the operations
6 performed by improved equi-angle interpolator 314 are simpler (i.e. less
7 computationally intensive) than those performed by interpolator 214.

8 Streak suppression filter 318 receives the equi-angle projections generated
9 by equi-angle interpolator 314 and generates therefrom streak corrected projections
10 which are in turn applied to isocenter interpolator 316. Streak suppression filter
11 318 suppresses high amplitude, high spatial frequency components from the
12 projections so as to reduce streak artifacts in the resulting tomograms. A version
13 of streak suppression filter 318 that is useful for CZA scanning is described in U.S.
14 Patent Application Serial No. 08/587,468, filed January 17, 1996 and entitled
15 STREAK SUPPRESSION FILTER FOR USE WITH COMPUTED
16 TOMOGRAPHY SYSTEM (Attorney Docket No. ANA-081), which is hereby
17 incorporated by reference.

18 Figure 17 shows a block diagram of streak suppression filter 318
19 constructed according to the invention. Filter 318 receives the projections
20 generated by equi-angle interpolator 316. Each of these projections include N data
21 points D:1 through D:N. From these data points, streak suppression filter 318
22 generates a set of streak corrected data points SC:1 through SC:N and these data
23 points are applied to isocenter interpolator 316. Filter 318 includes a spatial filter
24 410, a set of N threshold devices 420:1 through 420:N, and a set of N adders 430:1
25 through 430:N. The spatial filter 410 receives all the data points D:i, for all i from
26 one to N. For every data point D:i the spatial filter generates a high frequency data
27 point HF:i and a low frequency data point LF:i. The high and low frequency data
28 points HF:i and LF:i are representative of the spatial high and spatial low
29 frequency content, respectively, of a neighborhood of data points D:i-x/2 to
30 D:i+x/2 around the data point D:i, where x defines the size of the neighborhood.
31 Each high frequency data point HF:i is applied to a corresponding threshold device

1 420:i, for all i from one to N. The threshold device 420:i generates a clipped data
2 point and applies this data point to one input terminal of the adder 430:i, for all i
3 from one to N. The low frequency data point LF:i is applied to the other input
4 terminal of the adder 430:i, for all i from one to N. The adder 430:i adds the data
5 points present at its two input terminals to generate the streak corrected data point
6 SC:i, for all i from one to N.

7 Spatial filter 410 normally generates the low frequency data point LF:i by
8 applying a low pass filter to the neighborhood of data points around the data point
9 D:i, and normally generates the high frequency data point HF:i by subtracting the
10 low frequency data point LF:i from the data point D:i. When the high and low
11 frequency data points are generated in this manner, the data point D:i may be
12 exactly recovered by summing the high and low frequency data points HF:i and
13 LF:i.

14 The threshold devices 420:i generate the clipped data points by thresholding
15 the high frequency data points, or by compressing the high frequency data points,
16 so as to reduce high amplitude, high spatial frequency portions of the streak
17 corrected projections. When the high frequency data point HF:i is of a relatively
18 low amplitude, the threshold device 420:i generates its clipped data point so that it
19 is exactly equal to the high frequency data point HF:i. In this case, adder 430:i
20 generates a streak corrected data point SC:i that is identical to the original data
21 point D:i (because the adder 430:i sums the low frequency data point LF:i and the
22 clipped data point generated by the threshold device 420:i, and this clipped data
23 point is equal to the high frequency data point HF:i). However, when the high
24 frequency data point HF:i is of a relatively large amplitude, the threshold device
25 420:i generates its clipped data point so that its amplitude is lower than that of the
26 high frequency data point HF:i. In this case, the adder 430:i generates the streak
27 corrected data point SC:i so that it is not identical to the data point D:i. Rather, the
28 high amplitude, high spatial frequency components in the neighborhood of data
29 points around the data point D:i are suppressed to generate the streak corrected data
30 point SC:i. So in general, the streak suppression filter suppresses high amplitude,
31 high frequency components.

The above-referenced U.S. Patent Application Serial No. 08/587,468, essentially describes the spatial filter 410 as generating the low frequency data point LF:i as a weighted average of the neighborhood of data points around the data point D:i according to the following Equation (12).

$$LF:i = \sum_{j=-x/2}^{x/2} a:j * D:(i-j) \quad (12)$$

Streak suppression filter 318, when using Equation (12), works well for suppressing streaks in CZA scan data. However, when filter 318 operates in this fashion, it tends to introduce unwanted artifacts into tomograms generated from CSH scan data. As stated above, there tends to be a discrepancy between odd data points and even data points in any single parallel beam projection generated during a helical scan, and this discrepancy appears as high frequency noise. As a result of this high frequency noise, when streak suppression filter 318 operates as discussed above, virtually every high frequency data point is above threshold and is compressed by the threshold devices 420:i. However, this compression is introduced as a result of the patient motion occurring during a helical scan rather than as a result of high contrast (streak artifact generating) features in the patient.

In the preferred embodiment of improved helical streak suppression filter 318, spatial filter 410 generates odd low and high frequency data points LF:2i+1 and HF:2i+1, respectively, using only odd data points, and generates even low and high frequency data points LF:2i and HF:2i, respectively, using only even data points. For example, spatial filter 410 may generate the low frequency data points LF:i according to the following Equation (13).

$$LF:i = \sum_{j=-x/2}^{x/2} a:j * D:i-2j \quad (13)$$

In this fashion, improved helical streak suppression filter 318 avoids combining data from even and odd data points in a single projection and thereby prevents the patient motion inherent in any helical scan from corrupting the operation of the filter 318. When streak suppression filter 318 operates in this

1 fashion, it responds to streak producing structures in the patient (i.e., high contrast
2 features) rather than to patient motion, and therefore tends to reduce artifacts in the
3 resulting tomograms generated from CSH scan data.

4 The streak corrected data points generated by filter 318 are then applied to
5 improved helical isocenter interpolator 316 (shown in Figure 16). Isocenter
6 interpolator 316 generates isocenter projections from the streak corrected
7 projections. As illustrated in Figure 15, each of the isocenter projections 260
8 generated by interpolator 316 includes a set of data points C_i . However, improved
9 isocenter interpolator 316 does not generate the data points C_i according to the
10 above Equation (11) as does interpolator 216. Rather, interpolator 316 generates
11 the data points C_i according to the following Equation (14).

$$12 \quad C:i = \sum_{j=-x/2}^{x/2} b:j * D:i-2j \quad (14)$$

13 Basically, Equation (11) is unsatisfactory because it generates each data
14 point $C:i$ as a weighted average of odd and even data points. As was stated above,
15 combining information from odd and even data points in this fashion tends to
16 introduce artifacts into the tomograms. Therefore, improved isocenter interpolator
17 316 preferably generates each data point $C:i$ as a weighted average of a
18 neighborhood of odd data points, or as a weighted average of a neighborhood of
19 even data points according to the above Equation (14). This form of isocenter
20 interpolation reduces artifacts in the resulting tomograms generated by CSH
21 scanning. In one preferred embodiment, the weights $b:i$ are selected so that the
22 data points $C:i$ are generated according to a six point Lagrange interpolation
23 (otherwise known as Everett interpolation). Six point Lagrange interpolation is
24 discussed in detail in, for example, *Handbook of Mathematical Functions*, edited by
25 M. Abramowitz and I. A. Stegun, Dover Publications, New York (1970).

26 While scanner 300 (shown in Figure 16) is a preferred embodiment of the
27 invention, those skilled in the art will appreciate that many variations of scanner
28 300 are also embraced within the invention. For example, many other types of
29 filters and devices are normally included in a CT scanner. By way of example, the
30 scanner would normally include a DAS disposed between the detector system and

1 the helical weighting system. Many other types of filters may also be included,
2 such as filters that perform temperature compensation, or afterglow compensation.
3 Also, while the preferred scanner includes the helical weighting system 210 that
4 applies the HA scan weights to the projection data, other types of weighting
5 systems, such as prior art weighting systems, may be used and the equi-angle
6 interpolator 314, streak suppression filter 318, and isocenter interpolator 316 may
7 each be used to improve the quality of the resulting tomograms. Also, while
8 detector systems with a quarter detector offset have been primarily discussed, those
9 skilled in the art that the invention may readily be adapted for use with detector
10 systems characterized by other types of offsets. Further, while the invention has
11 been discussed in connection with CSH scanning, those skilled in the art will
12 appreciate that the invention may be easily adapted for use with non-constant speed
13 helical scanning.

14 Since certain changes may be made in the above apparatus without departing
15 from the scope of the invention herein involved, it is intended that all matter
16 contained in the above description or shown in the accompanying drawing shall be
17 interpreted in an illustrative and not a limiting sense.

What is Claimed is:

1 1. A method of acquiring projection data on a tomographic imaging system
2 of the type comprising (a) means for acquiring data from a series of fan beam
3 projections of an imaged object at a plurality of angles as a source of x-rays
4 revolves about a z-axis about a mechanical center of rotation within an imaging
5 plane, (b) means for translating the imaged object and imaging plane relative to one
6 another along the z-axis, wherein the each of the fan beam projections subtends
7 maximum angles ϕ_1 and ϕ_2 respectively with respect to a line connecting the apex
8 of the fan beam with the mechanical center of rotation, wherein ϕ_1 and ϕ_2 are
9 different, said method comprising the steps of:

10 identifying a slice plane at a position along the z-axis relative to the imaged
11 object;

12 translating the object and imaging plane relative to one another along the z-
13 axis to move the slice plane through the imaging plane;

14 acquiring a tomographic set of data comprised of data from a plurality of
15 projections; and

16 reconstructing a tomographic image at the slice plane.

1 2. The method of claim 1, further including the step of weighting said
2 projections prior to the step of reconstructing said tomographic image.

1 3. The method of claim 2, wherein the step of reconstructing the
2 tomographic image includes the step of using filtered back projection to reconstruct
3 said tomographic image.

1 4. The method of claim 2, wherein the step of acquiring a tomographic set
2 of data includes the step of acquiring at least 720 degrees of fan beam projections,
3 and wherein the step of reconstructing a tomographic image includes the step of
4 using the 720 degrees of fan beam projections to reconstruct the tomographic
5 image.

1 5. The method of claim 4, wherein the step of reconstructing the
2 tomographic image includes the step of back projecting 720 degrees of fan beam
3 projections.

1 6. The method of claim 4, wherein the step of reconstructing the
2 tomographic image includes the steps of combining fan beam projections displaced
3 by 360 degrees and back projecting 360 degrees of combined fan beam projections.

1 7. The method of claim 4, wherein the system includes a plurality of
2 detectors, and ϕ describes the angle subtended by a detector and the line connecting
3 the apex of the fan with the mechanical center-of-rotation, ϕ_{\max} is the greater of the
4 two values of ϕ_1 and ϕ_2 and where ϕ_{\min} is the lesser of the two values of ϕ_1 and ϕ_2 ,
5 the method further comprising the steps of using a first weighting scheme for
6 weighting data acquired by detectors with $|\phi| < \phi_{\min}$ and using a second weighting
7 scheme for data acquired by detectors with $\phi_{\min} < \phi < \phi_{\max}$.

1 8. The method of claim 7, wherein the step of using the first weighting
2 scheme includes the step of setting projections to zero over a range of 360 degrees
3 minus $4\phi_{\max}$.

1 9. The method of claim 7, wherein the step of using the first weighting
2 scheme includes the step of setting projections to zero over a range of 360 degrees.

1 10. The method of claim 7, wherein the step of using the first weighting
2 scheme includes the step of using weights corresponding to linear interpolation of
3 data.

1 11. The method of claim 7, wherein the step of using the first weighting
2 scheme includes the step of using weights corresponding to linear interpolation and
3 linear extrapolation of data.

1 12. The method of claim 7, wherein the step of using the second weighting
2 scheme includes the step of using weights corresponding to linear interpolation of
3 data.

1 13. The method of claim 7, wherein the step of using the second weighting
2 scheme includes the step of using weights corresponding to linear interpolation and
3 linear extrapolation of data.

1 14. The method of claim 7, wherein the steps of using the first and second
2 weighting schemes includes the step of blending said first and second weighting
3 schemes for $|\phi| < \phi_{\min}$.

1 15. The method of claim 14, wherein the step of blending includes the step
2 of using linear blending functions.

1 16. The method of claim 14, wherein the step of blending includes the step
2 of using quadratic blending functions.

1 17. The method of claim 14, wherein the step of blending is uses over the
2 angle subtended by ten detectors.

1 18. The method of claim 1, further including the step of converting said fan
2 beam projections to parallel projections prior to the step of reconstructing the
3 tomographic image.

1 19. The method of claim 18, wherein the step of converting includes the
2 steps of interpolating data so as to form parallel projections with equal spacing in
3 the detector direction.

1 20. The method of claim 19, wherein the step of interpolating data includes
2 the step of using data acquired by every other detector.

1 21. The method of claim 18, further including the step of interleaving
2 parallel projections displaced by 180 degrees prior to the step of reconstructing the
3 tomographic image.

1 22. The method of claim 21, wherein the step of interleaving parallel
2 projections includes the step of nonlinearly filtering data of the parallel projections.

1 23. The method of claim 22, wherein the step of nonlinearly filtering
2 includes the step of using data acquired from every other detector.

1 24. The method of claim 18, further including the step of weighting the fan
2 beam projections prior to the step of converting said fan beam projections to
3 parallel projections.

1 25. The method of claim 18, further including the step of weighting the
2 parallel projections prior to the step of reconstructing the tomographic image.

1 26. A tomographic imaging system for creating a tomographic image of an
2 object, said system comprising:

3 (a) means for defining a plurality of fan beam projections as a source of x-
4 rays revolves around a z-axis about a mechanical center of rotation within an
5 imaging plane, wherein each of the fan beam projections subtends maximum angles
6 ϕ_1 and ϕ_2 respectively with respect to a line connecting the apex of the fan beam
7 with the mechanical center of rotation, wherein ϕ_1 and ϕ_2 are different;

8 (b) means for translating the object and imaging plane relative to one
9 another along the z-axis;

10 (c) means for acquiring a tomographic project set of data from a series of
11 fan beam projections of the imaged object at a plurality of angles about the z-axis
12 as the source revolves around the z-axis about a mechanical center of rotation, and
13 the object and imaging plane are translated relative to one another; and

14 (d) means for reconstructing the tomographic image from the acquired data.

1 27. The system of claim 26, wherein said means for translating the object
2 and the imaging plane relative to one another includes means for identifying a slice
3 plane at a position along the z-axis relative to the imaged object; and means for
4 translating the object and imaging plane relative to one another along the z-axis to
5 move the slice plane through the imaging plane; and said means for reconstructing
6 a tomographic image from the acquired data includes means for reconstructing the
7 tomographic image at the slice plane.

1 28. The system of claim 27, further including means for weighting said
2 projections prior to reconstructing said tomographic image.

1 29. The system of claim 27, wherein the means for reconstructing the
2 tomographic image includes means for filtered back projecting data to reconstruct
3 said tomographic image.

1 30. The system of claim 27, wherein the means for acquiring a
2 tomographic project set of data includes means for acquiring at least 720 degrees of
3 fan beam projections, and wherein means for reconstructing a tomographic image
4 includes means for using the 720 degrees of fan beam projections to reconstruct the
5 tomographic image.

1 31. The system of claim 30, wherein the means for reconstructing the
2 tomographic image includes means for back projecting 720 degrees of fan beam
3 projections.

1 32. The system of claim 30, wherein the means for reconstructing the
2 tomographic image includes means for combining fan beam projections displaced
3 by 360 degrees and means for back projecting 360 degrees of combined fan beam
4 projections.

1 33. The system of claim 30, further including a plurality of detectors, and

2 ϕ describes the angle subtended by a detector and the line connecting the apex of
3 the fan with the mechanical center-of-rotation, ϕ_{\max} is the greater of the two values
4 of ϕ_1 and ϕ_2 and where ϕ_{\min} is the lesser of the two values of ϕ_1 and ϕ_2 , the system
5 further comprising means for using a first weighting scheme for weighting data
6 acquired by detectors with $|\phi| < \phi_{\min}$ and means for using a second weighting
7 scheme for data acquired by detectors with $\phi_{\min} < \phi < \phi_{\max}$.

1 34. The system of claim 33, wherein the means for using the first
2 weighting scheme includes means for setting projections to zero over a range of
3 360 degrees minus $4\phi_{\max}$.

1 35. The system of claim 33, wherein the means for using the first
2 weighting scheme includes means for setting projections to zero over a range of
3 360 degrees.

1 36. The system of claim 33, wherein the means for using the first
2 weighting scheme includes means for using weights corresponding to linear
3 interpolation of data.

1 37. The system of claim 33, wherein the means for using the first
2 weighting scheme includes means for using weights corresponding to linear
3 interpolation and linear extrapolation of data.

1 38. The system of claim 33, wherein the means for using the second
2 weighting scheme includes means for using weights corresponding to linear
3 interpolation of data.

1 39. The system of claim 33, wherein the means for using the second
2 weighting scheme includes means for using weights corresponding to linear
3 interpolation and linear extrapolation of data.

1 40. The system of claim 33, wherein the means for using the first and
2 second weighting schemes includes means for blending the first and second
3 weighting schemes for $|\phi| < \phi_{\min}$.

1 41. The system of claim 40, wherein the means for blending includes
2 means for using linear blending functions.

1 42. The system of claim 40, wherein the means for blending includes
2 means for using quadratic blending functions.

1 43. The system of claim 40, wherein the means for blending is used over
2 the angle subtended by ten detectors.

1 44. The system of claim 27, further including means for converting said
2 fan beam projections to parallel projections prior to reconstructing the tomographic
3 image.

1 45. The system of claim 44, wherein the means for converting includes
2 means for interpolating data so as to form parallel projections with equal spacing in
3 the detector direction.

1 46. The system of claim 45, wherein the means for interpolating data
2 includes means for using data acquired by every other detector.

1 47. The system of claim 44, further including means for interleaving
2 parallel projections displaced by 180 degrees prior to the step of reconstructing the
3 tomographic image.

1 48. The system of claim 47, wherein the means for interleaving parallel
2 projections includes means for nonlinearly filtering data of the parallel projections.

1 49. The system of claim 48, wherein the means for nonlinearly filtering
2 includes means for using data acquired from every other detector.

1 50. The system of claim 44, further including means for weighting the fan
2 beam projections prior converting said fan beam projections to parallel projections.

1 51. The system of claim 44, further including means for weighting the
2 parallel projections prior to reconstructing the tomographic image.

1/8

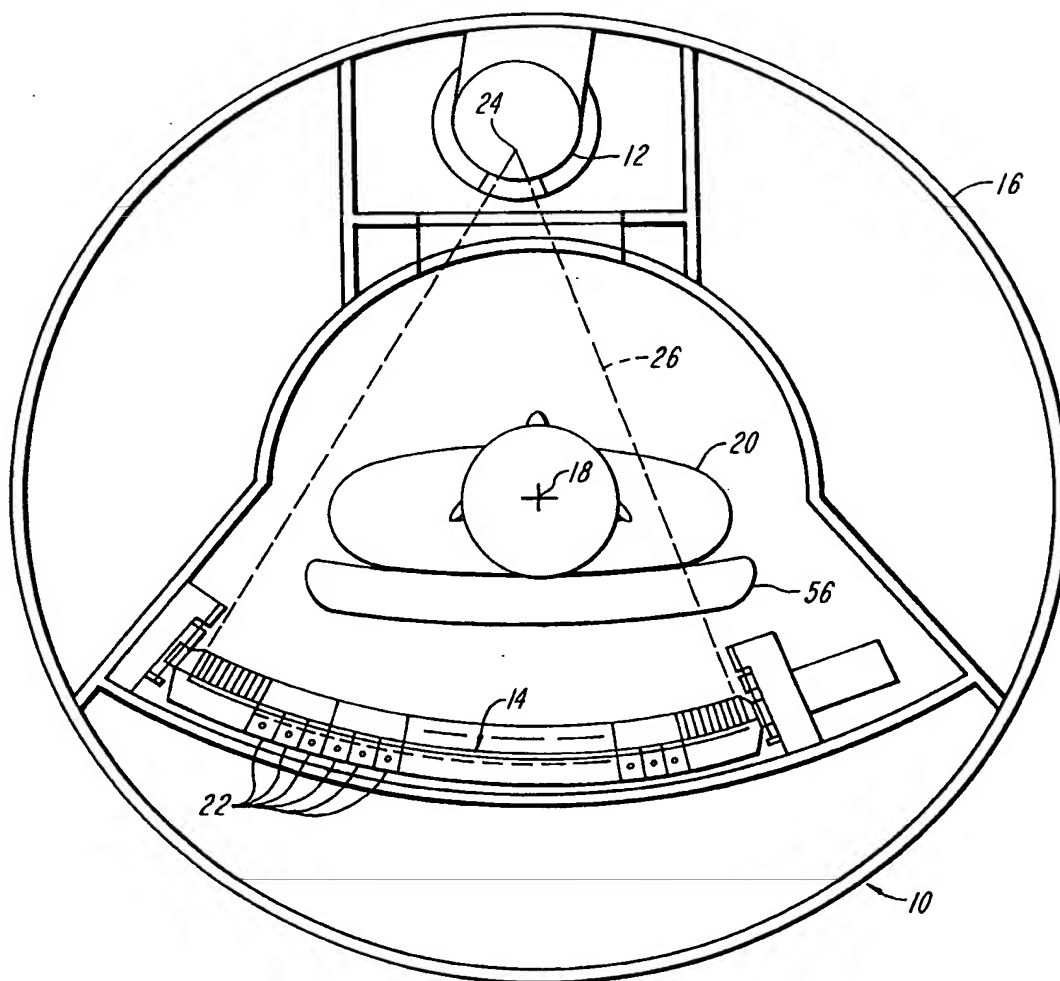


FIG. 1
(PRIOR ART)

2/8

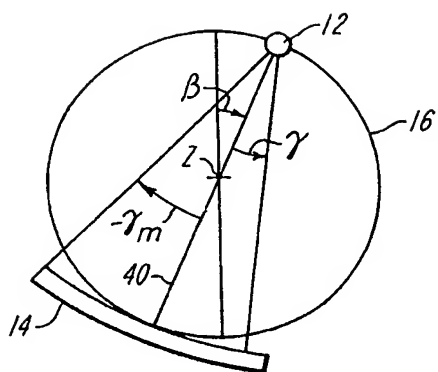


FIG. 2
(PRIOR ART)

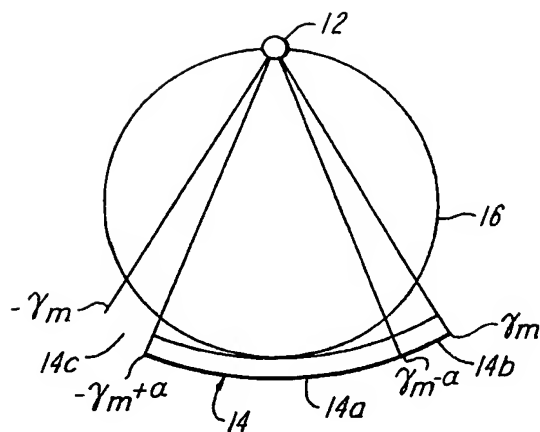


FIG. 6
(PRIOR ART)

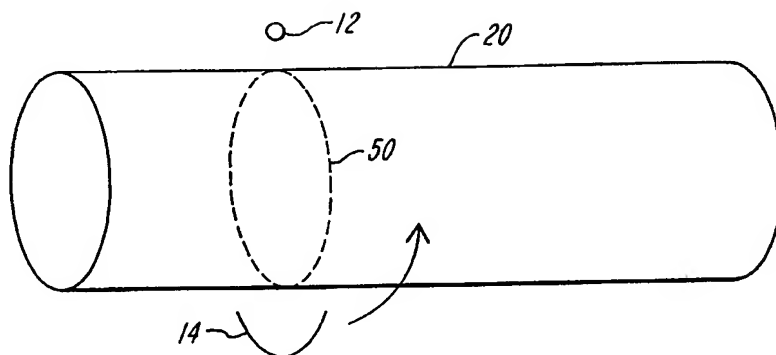


FIG. 3A
(PRIOR ART)

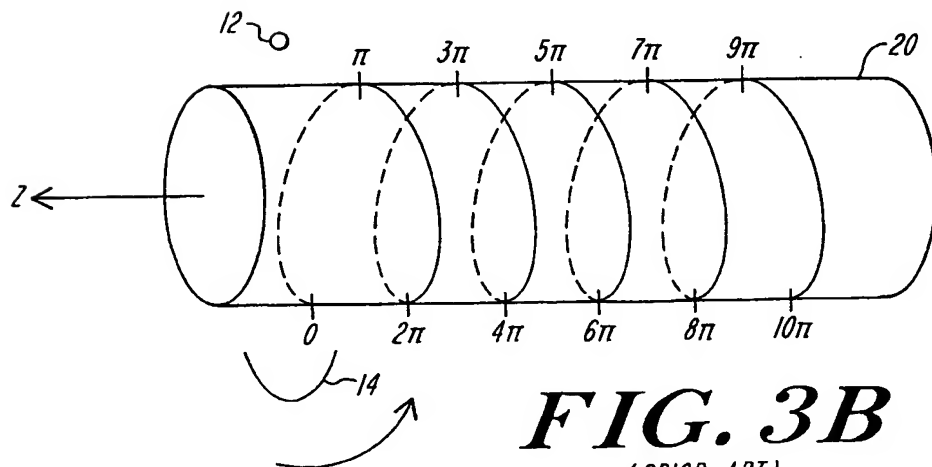


FIG. 3B
(PRIOR ART)

3/8

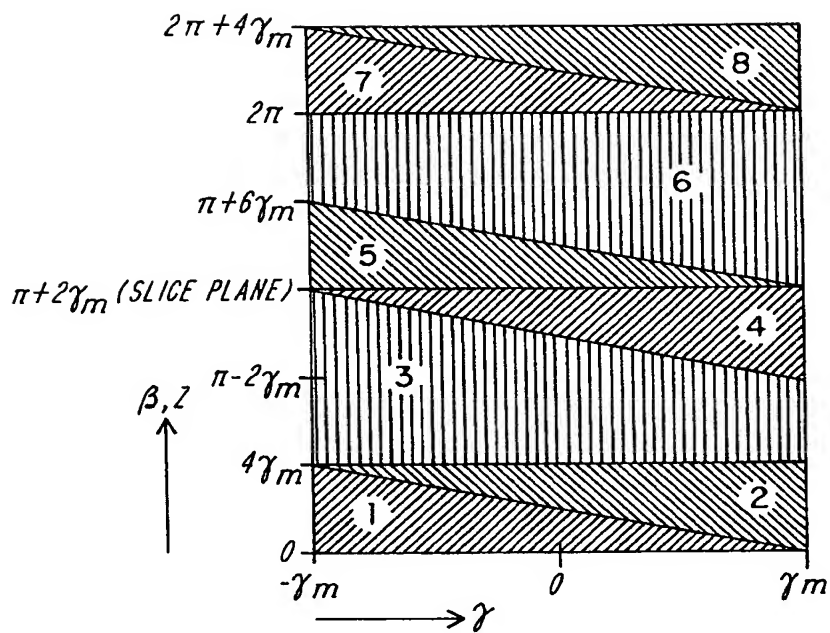


FIG. 4
(PRIOR ART)

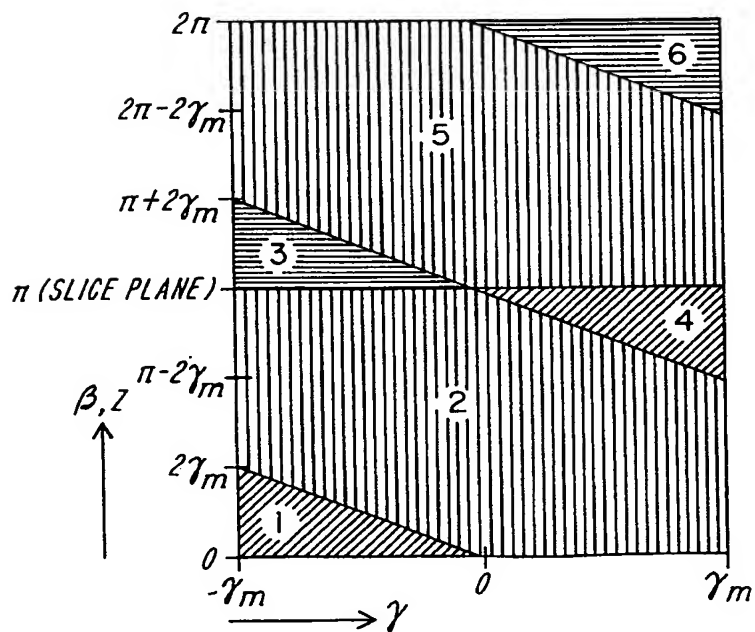


FIG. 5
(PRIOR ART)

4/8

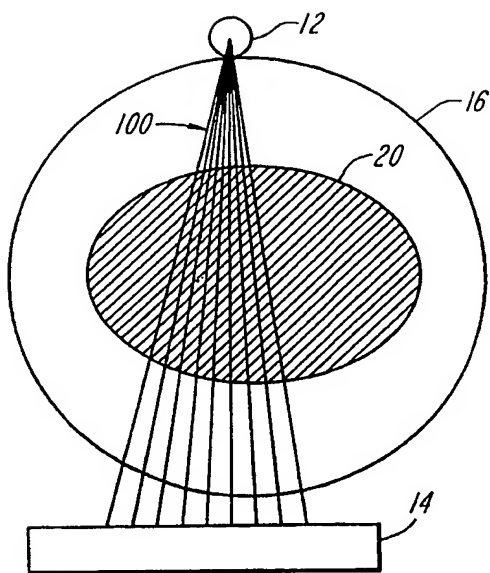


FIG. 7A
(PRIOR ART)

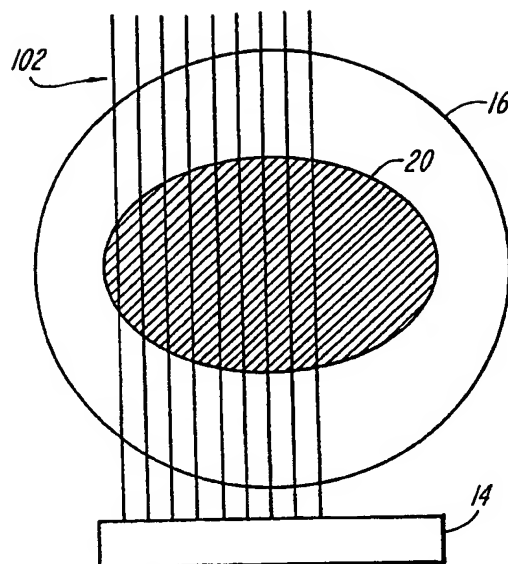


FIG. 7B
(PRIOR ART)

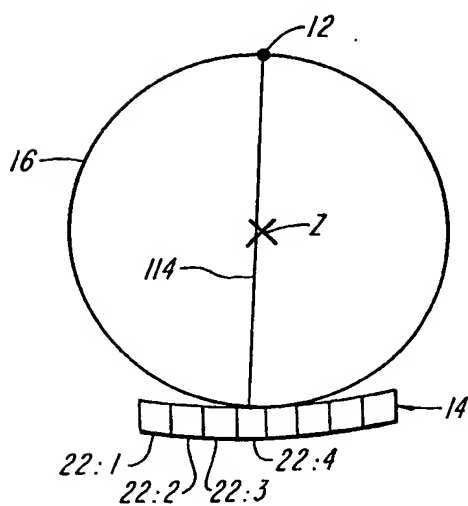


FIG. 8A
(PRIOR ART)

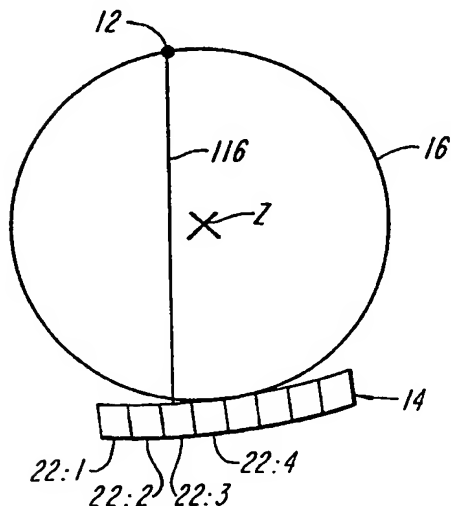
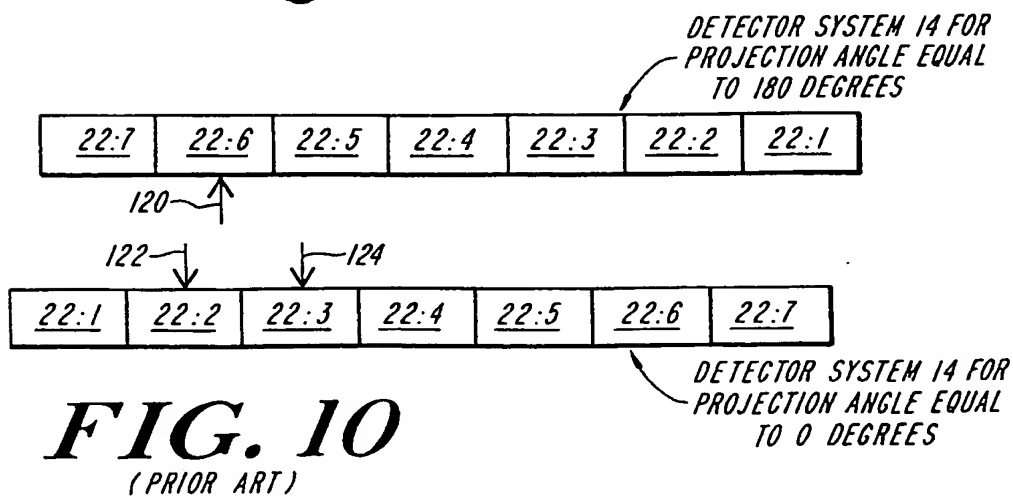
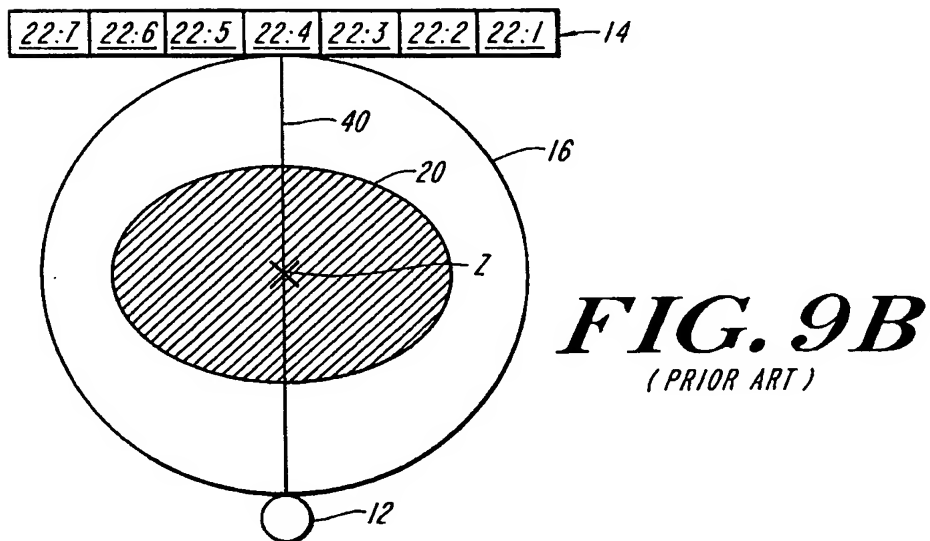
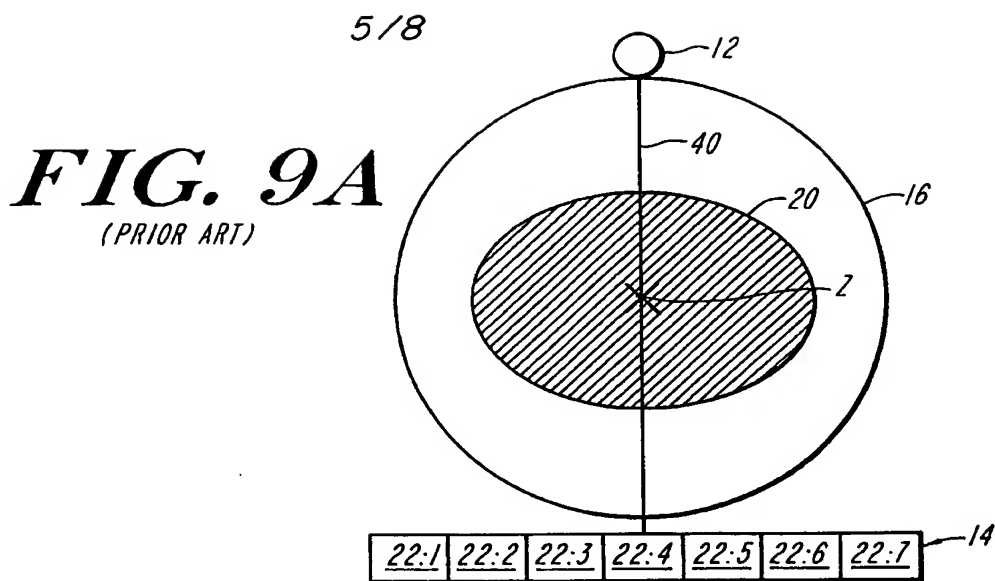
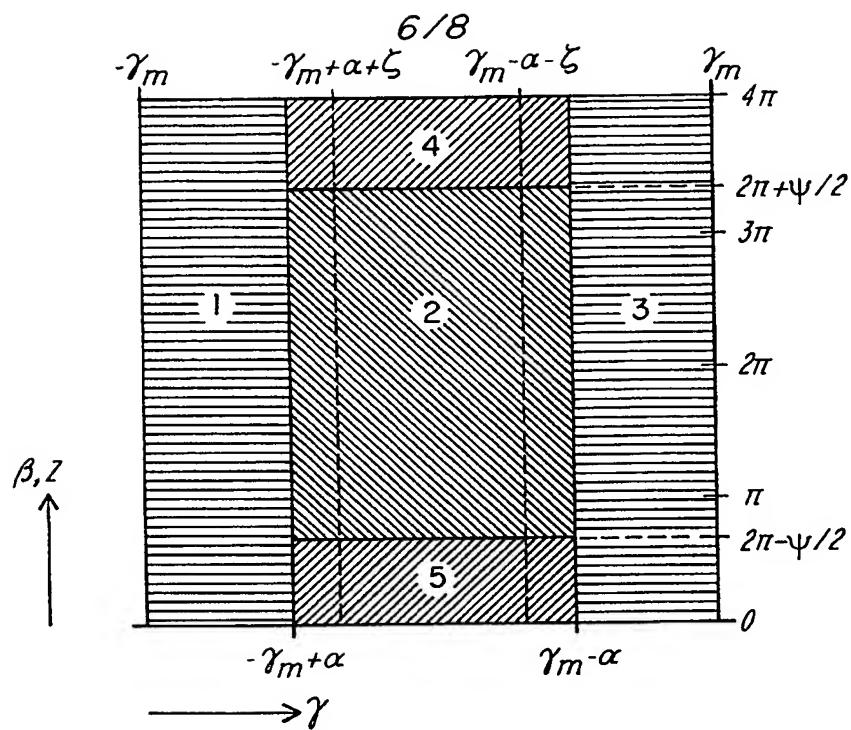
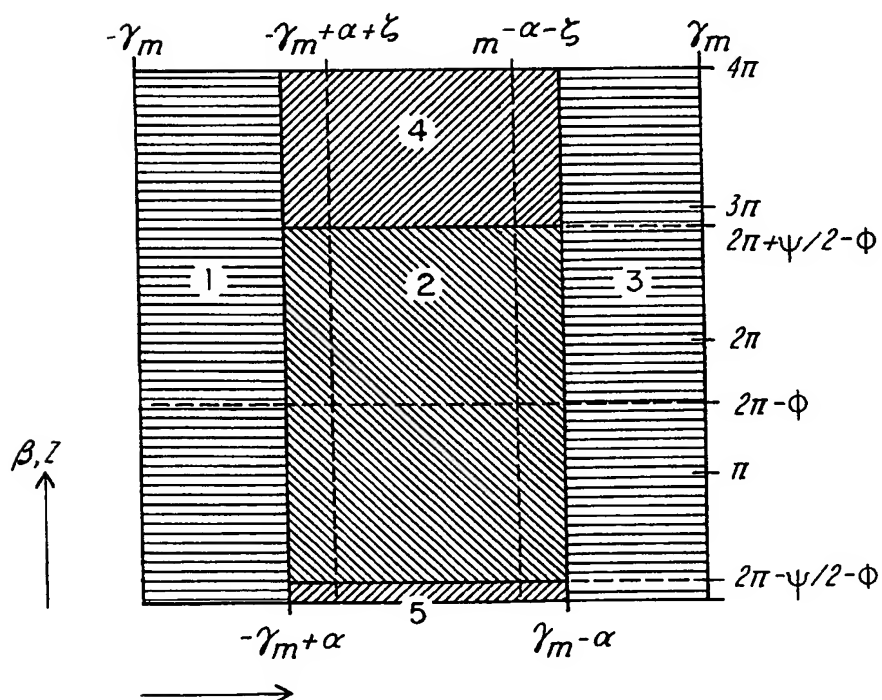
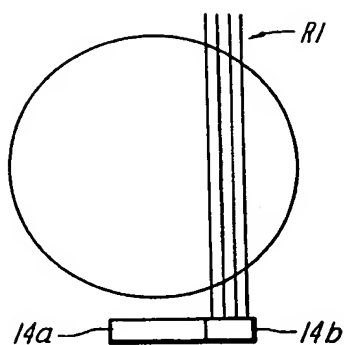
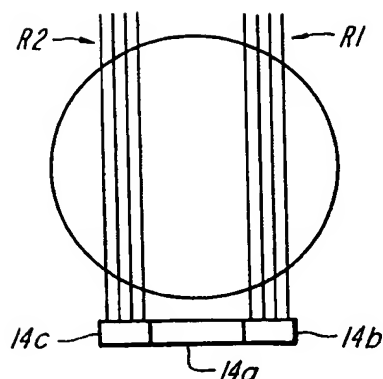
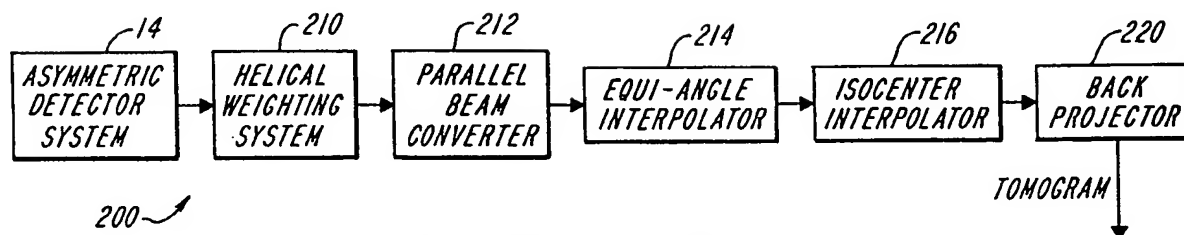
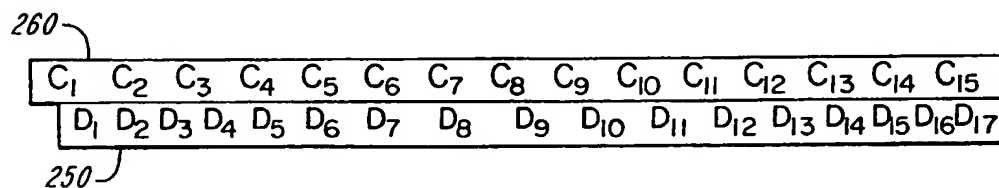


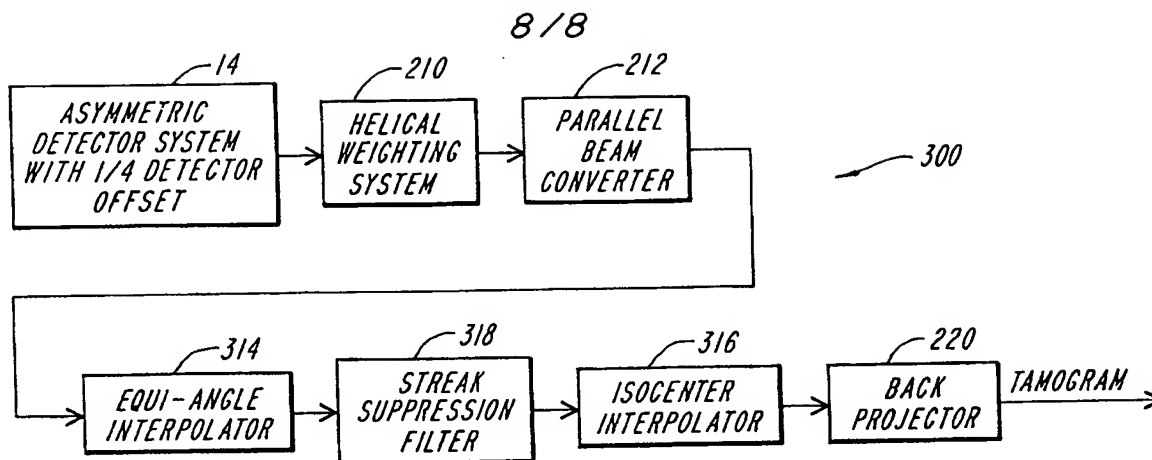
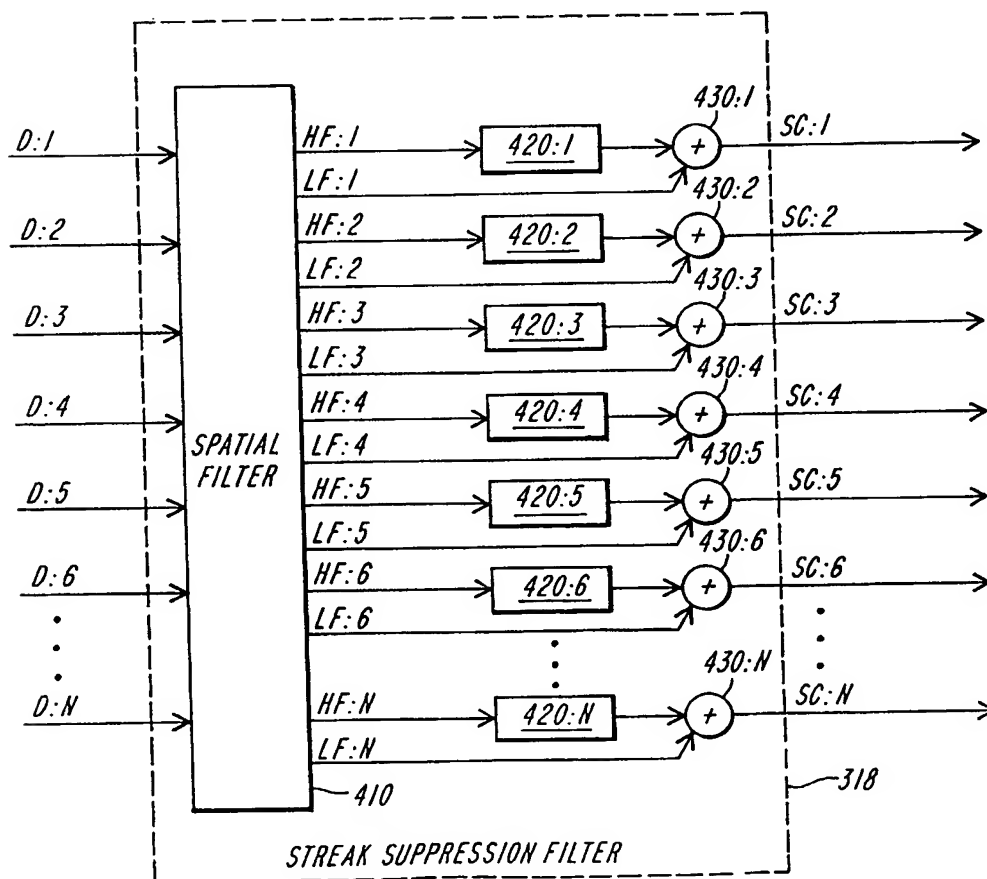
FIG. 8B
(PRIOR ART)



**FIG. 11****FIG. 12**

7/8

**FIG. 13A****FIG. 13B****FIG. 14****FIG. 15**

**FIG. 16****FIG. 17**

INTERNATIONAL SEARCH REPORT

International application No.
PCT/US97/21036

A. CLASSIFICATION OF SUBJECT MATTER

IPC(6) : A 61 B 6/03

US CL : 378/15, 19

According to International Patent Classification (IPC) or to both national classification and IPC

B. FIELDS SEARCHED

Minimum documentation searched (classification system followed by classification symbols)

U.S. : 378/4, 15, 19, 901

Documentation searched other than minimum documentation to the extent that such documents are included in the fields searched

Electronic data base consulted during the international search (name of data base and, where practicable, search terms used)

APS

search terms: computed tomography, angle, detector, helical, spiral

C. DOCUMENTS CONSIDERED TO BE RELEVANT

Category*	Citation of document, with indication, where appropriate, of the relevant passages	Relevant to claim No.
A	US 4,417,353 A (GROH ET AL.) 22 November 1983 (22-11-83)	1-51
A, P	US 5,668,851 A (DOBBS) 16 September 1997 (16-09-97)	1-51
A, P	US 5,680,427 A (DOBBS ET AL.) 21 October 1997 (21-10-97)	1-51

☐ Further documents are listed in the continuation of Box C. ☐ See patent family annex.

* Special categories of cited documents:	*T* later document published after the international filing date or priority date and not in conflict with the application but cited to understand the principle or theory underlying the invention
A document defining the general state of the art which is not considered to be of particular relevance	*X* document of particular relevance; the claimed invention cannot be considered novel or cannot be considered to involve an inventive step when the document is taken alone
B earlier document published on or after the international filing date	*Y* document of particular relevance; the claimed invention cannot be considered to involve an inventive step when the document is combined with one or more other such documents, such combination being obvious to a person skilled in the art
L document which may throw doubts on priority claim(s) or which is cited to establish the publication date of another citation or other special reason (as specified)	*A* document member of the same patent family
O document referring to an oral disclosure, use, exhibition or other means	
P document published prior to the international filing date but later than the priority date claimed	

Date of the actual completion of the international search

10 FEBRUARY 1998

Date of mailing of the international search report

02 MAR 1998

Name and mailing address of the ISA/US
Commissioner of Patents and Trademarks
Box PCT
Washington, D.C. 20231

Facsimile No. (703) 305-3230

Authorized officer

DAVID VERNON BRUCE

Telephone No. (703) 308-0956

THIS PAGE BLANK (USPTO)